



Review

Adsorption of polycyclic aromatic hydrocarbons from wastewater using graphene-based nanomaterials synthesized by conventional chemistry and green synthesis: A critical review

Ruth Nóbrega Queiroz^a, Patrícia Prediger^b, Melissa Gurgel Adeodato Vieira^{a,*}

^a Process and Product Development Department, School of Chemical Engineering, University of Campinas – UNICAMP, Albert Einstein Avenue, 500, 13083-852 Campinas, São Paulo, Brazil

^b School of Technology, University of Campinas – UNICAMP, 13484-332 Limeira, São Paulo, Brazil



ARTICLE INFO

Editor: Dr. H. Artuto

Keywords:

PAHs
Remediation
Green nanomaterials
Carbon-based nanomaterials
Graphene

ABSTRACT

Polycyclic aromatic hydrocarbons (PAHs) are organic pollutants formed mainly by the incomplete combustion of organic matter, such as oil, gas and coal. The presence of PAHs can cause irreparable damage to the environment and living beings, which has generated a global concern with the short and long term risks that the emission of these pollutants can cause. Many technologies have been developed in the last decades aiming at the identification and treatment of these compounds, mainly, the PAHs from wastewater. This review features an overview of studies on the main methods of PAHs remediation from wastewater, highlighting the adsorption processes, through the application of different adsorbent nanomaterials, with a main focus on graphene-based nanomaterials, synthesized by conventional and green routes. Batch and fixed-bed adsorptive processes were evaluated, as well as, the mechanisms associated with such processes, based on kinetic, equilibrium and thermodynamic studies. Based on the studies analyzed in this review, green nanomaterials showed higher efficiency in removing PAHs than the conventional nanomaterials. As perspectives for future research, the use of green nanomaterials has shown to be sustainable and promising for PAHs remediation, so that further studies are needed to overcome the possible challenges and limitations of green synthesis methodologies.

1. Introduction

Industrial wastewater, including oil from the oil sector, has a high pollutant potential, due to the presence of aromatic pollutants, such as Polycyclic Aromatic Hydrocarbons (PAHs). Based on this, some methodologies for treating industrial effluents have been applied to remove such contaminants from ecosystems, thus seeking to meet socio-environmental and economic demands. The presence of PAHs in wastewater represents a major source of concern for the industrial sector, since they can cause irreparable damage to the environment and to humans, due to their high toxic and polluting potential (Beyer et al., 2020).

Many studies have been developed aiming to optimize the wastewater treatment processes, such as bioremediation methods, which are based on the application of microorganisms that perform the biodegradation of polluting compounds through their microbial activity (Qi et al., 2017). Other treatment methods can be applied, such as chemical

oxidation, coagulation-flocculation, membrane separation and adsorption (Scurtu, 2009). Among these technologies, the adsorptive processes have been widely used, as they present low production cost, high selectivity, applicability in low concentrations, they can be applied in continuous and batch processes. In addition to this, adsorbent materials can be regenerated and reused in other adsorptive cycles (Nasuhoglu et al., 2012).

Some graphene-based materials have attracted the attention of researchers regarding their use for the PAHs adsorption from wastewater. Graphene-based materials have some characteristics, such as high surface area, mechanical resistance and low-cost production, which facilitate their use for the treatment of effluents by adsorption processes (Chen and Huang, 2020).

The application of green nanoadsorbents, produced by means of natural agents (plants extracts, fruits and microorganisms), for the removal of organic pollutants, like PAHs, from the environment, has been the main focus of some studies, due to their capacity to minimize

* Corresponding author.

E-mail address: melissag@unicamp.br (M.G.A. Vieira).

<https://doi.org/10.1016/j.jhazmat.2021.126904>

Received 28 May 2021; Received in revised form 26 July 2021; Accepted 11 August 2021

Available online 13 August 2021

0304-3894/© 2021 Elsevier B.V. All rights reserved.

the toxic effects caused by the use of chemical reagents in the conventional synthesis processes of adsorbents (Bolade et al., 2020).

In this context, this review aims to critically address researches about PAHs removal from wastewater, using different remediation technologies, but with a main focus on the adsorption of PAHs by means of graphene-based materials, synthesized by conventional and green methods. Therefore, the main topics that will be covered in this review are: (i) Overview of Polycyclic Aromatic Hydrocarbons, sources and removal techniques; (ii) General concepts of adsorption, kinetics, isotherms, thermodynamics and fixed-bed applications; (iii) Nanomaterial-based adsorbents; (iv) Adsorption of PAHs by graphene-based nanomaterials; (v) Green synthesized nanomaterials for PAHs removal.

2. Research strategy

As a research strategy for the development of this review, initially, a wide bibliographic search was carried out through the scientific document bases Royal Society of Chemistry (RSC), ScienceDirect and American Chemical Society (ACS). The search was carried out using as keywords, "PAHs removal from wastewater", "PAHs adsorption", "graphene-based nanomaterials", "green nanomaterials", "green nanomaterials for PAHs removal" and other similar terms. As exclusion criteria, the articles were selected between the years 2008–2021, and considering only indexed articles written in English. To identify the articles of interest, a combination of terms was used, which were called 'Search Outline Strategies', as shown in Table 1, in which the 'base terms' on the left were combined with the 'complementary terms' on the right.

Applying the established search strategy, an average of 8170 articles were found, adding up all the databases used. After analyzing the titles, 200 articles were selected for reading the abstracts. After analyzing the abstracts, the literature was selected to be discussed in the review based on its relevance to the subject and its references. At the end, a total of 65 articles were chosen, covering experimental and observational studies, which met the initially proposed criteria. It is important to highlight that this review emphasizes, mainly, the adsorption of PAHs by graphene-based nanomaterials (synthesized by conventional and green route) from wastewater. However, other PAHs remediation technologies have also been addressed. Fig. 1 graphically shows the number of documents published per year and the most applied methods for removing PAHs from wastewater, based on searches in the ScienceDirect, RSC and ACS databases.

3. Sources of Polycyclic aromatic hydrocarbons (PAHs)

Polycyclic aromatic hydrocarbons (PAHs) can be defined as nonpolar organic substances formed basically by carbon and hydrogen atoms. In general, PAHs are formed through incomplete combustion of organic matter and fossil fuels, such as gas, oil, coal, wood, smoked foods, among others (Abdel-Shafy and Mansour, 2016; Ghosal et al., 2016).

PAHs can be divided into two classifications: (LMW) low molecular weight PAHs and (HMW) high molecular weight PAHs. LMW PAHs have a central structure composed of two or three aromatic rings, for example, naphthalene, acenaphthene, fluorene, anthracene and phenanthrene. HMW PAHs have molecular structures composed of four or

Table 1
Search Outline Strategies used on the review.

Base terms	Complementary terms
PAHs	Wastewater Remediation technologies
Adsorption	Adsorbents Kinetics, isotherms and thermodynamics
Graphene	Fixed-bed Green
Nanomaterials	Synthesis

more aromatic rings, for example, fluoranthene, pyrene and benzo-fluoranthenes. LMW PAHs have greater volatility and solubility than HMW PAHs, which makes them break more easily than HMW PAHs. (Adeniji et al., 2018) (see Fig. S1 and Table S1).

The main sources of PAHs for the environment can be of natural (biological) or anthropogenic (pyrogenic and petrogenic) origins (see Fig. S2). Biological PAHs are those produced through the enzymatic activity of some types of plants and bacteria or formed through the degradation of organic matter. Some biological sources of PAHs are: volcanoes, enzymatic activity of bacteria and algae, degradation of plant matter and rocky sediments containing oil and gas (Abdel-Shafy and Mansour, 2016).

Pyrogenic PAHs are formed through a pyrolysis process, in which organic substances are exposed to high temperatures (350° to 1200 °C) in the absence of oxygen. They are usually formed through incomplete combustion of biomass and fossil fuels, and are found in greater concentrations in urban areas (Abdel-Shafy and Mansour, 2016; Masood et al., 2016).

PAHs can also be found in crude oil, which can form during the maturation process, or even in petroleum products, which can be called petrogenic PAHs. These PAHs can be found during the stages of transportation, storage and consumption of oil and its derivatives. Oil spills in oceans and rivers, leaks in storage tanks and emission of gases during transport, are among the main factors responsible for the increase in the concentration of petrogenic PAHs in the environment (Abdel-Shafy and Mansour, 2016; Nikitha et al., 2017).

Produced water (PW) is characterized as a by-product of the petrochemical industry, which can be used for reinjection in oil wells, to increase its production, or it can also be discarded after its treatment (Abdullahi et al., 2021). The concentration of PAHs in wastewater from petrogenic origin represents a major source of concern for the sector. Despite representing a small fraction (about 0.306%) of the composition of the PW, PAHs are considered risky components, due to their high toxic and polluting potential, which can last for many years in the ecosystems, and can cause irremediable damage to human health, due to their carcinogenic, genotoxic and mutagenic potential (Beyer et al., 2020; Mukhopadhyay et al., 2020).

4. Adsorption processes for PAHs removal

4.1. General concepts

Adsorption is characterized as a surface phenomenon, which is associated with factors such as the porous structure and the chemical properties of the adsorbent solid. Differences in molar mass, shape or polarity are the main factors that contribute to the separation of adsorbate from the fluid phase, as they allow the attachment of some molecules to the surface of the adsorbent material. The nature of the interactions between adsorbate and adsorbent influences the classification of adsorbent processes, which can be classified into two mechanisms, physical adsorption (physisorption) and chemical adsorption (chemisorption) (Marczewska and Marczewski, 2002).

The physisorption processes are reversible and occur at low temperatures, so that the bonds between the adsorbate and the adsorbent surface occur through relatively weak electrostatic interactions, being attributed to dipole-dipole, Van der Waals and π - π interactions, dispersion interactions and hydrogen bonding (Ruthven, 1984). The chemisorption processes are irreversible and, generally, occur at high temperatures, allowing chemical interactions to be established through the electronic transfer between the adsorbent surface and the adsorbate, generating changes in the chemical nature of the adsorbate (Lander, 1964; Muscat and Newns, 1978).

The adsorptive processes are operated in two main modes: batch flow and continuous flow systems. Batch adsorption is widely used to treat small volumes, often used on a pilot scale in laboratories. These systems are composed of a batch reactor containing a colloidal suspension of an

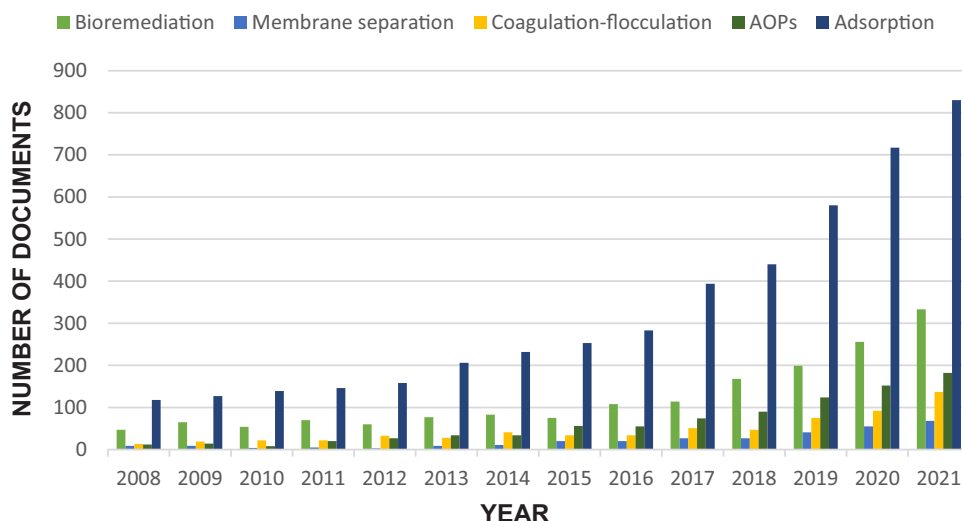


Fig. 1. Number of documents published per year, which address technologies for the removal of PAHs from wastewater, from 2008–2021, based on searches in the ScienceDirect, RSC and ACS databases.

adsorbent in the presence of an adsorbate that is mixed in a certain time. The effect of parameters such as temperature, adsorbate concentration, amount of adsorbent, agitation speed and particle size of the adsorbent are also evaluated, until the equilibrium condition is reached (Schweich and Sardin, 1981). Continuous adsorption systems are applied, generally, for industrial scale processes. Of all techniques used for the contact between adsorbate and the adsorbent in this processes, the fixed bed column of continuous flow is the most applied. In studies of continuous adsorption systems, parameters such as initial concentration of adsorbate, flow of adsorbate, column bed height, pH, particle size of the adsorbent, system temperature, breaking points and exhaustion, have their effect evaluated in column adsorptive processes (Gupta et al., 1998).

The schematic representation of the main types of adsorbents used for PAHs adsorption from wastewater is shown in Fig. 2. It is important to emphasize that, in this review, only carbon-based adsorbents will be addressed.

4.2. Adsorption kinetics

Adsorption kinetics studies are very important for the understanding of the mechanisms that control the adsorptive processes, as well as their limiting steps and the determination of the ideal process conditions. Factors such as pH, adsorbate concentration, temperature, size and specific surface area of the adsorbent, directly influence the adsorption kinetics (Ho and McKay, 1999). The main kinetic models applied to the study of the behavior of adsorbents, as well as, the mechanisms that control the adsorption, are the Pseudo-First Order (PFO), proposed by Lagergren (1898), and Pseudo-Second Order (PSO), proposed by Ho and McKay (1999), models. Table 2 displays the equations of the PFO and PSO models, as well as their linearized forms.

Ruiz et al. (2020) proposed the synthesis of an ecologically correct and low-cost production of material, aiming at the remediation of PAHs from water sources. In this study, chitosan granules were modified by means of FeO and TiO₂ through ionic cross-linking (Ch-FeO/TiO₂), in which FeO was synthesized by the coprecipitation method and TiO₂ by the green chemistry method. SEM, XRD, FTIR and BET techniques were used to characterize the obtained nanomaterial, then it was applied for

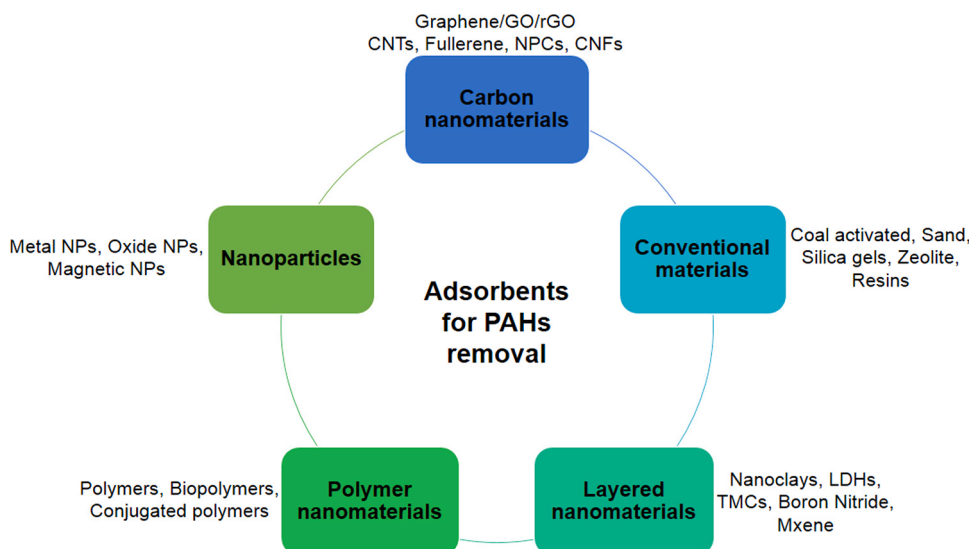


Fig. 2. Schematic representation of the types of adsorbents used for PAHs adsorption from wastewater.

Table 2

Kinetic models: Pseudo-First Order (PFO) and Pseudo-Second Order (PSO).

Kinetic model	Equation	Linearized form
PFO: Related with the adsorbent's adsorption capacity (Lagergren, 1898).	$q(t) = q_e(1 - e^{-k_1 t})$ (1)	$\ln(q_e - q(t)) = \ln q_e - k_1 t$ (2)
PSO: Related with the chemisorption of adsorbate in the adsorbent (Ho and McKay, 1999).	$q(t) = \frac{k_2 q_e^2 t}{1 + k_2 q_e t}$ (3)	$\frac{t}{q(t)} = \frac{1}{k_2 q_e^2} + \frac{t}{q_e}$ (4)

$q(t)$: adsorbate concentration on the adsorbent surface at time t (min) (mg g^{-1}), q_e : adsorbate concentration in equilibrium on the adsorbent surface (mg g^{-1}), k_1 : PFO rate constant (min^{-1}) and k_2 : PSO rate constant ($\text{g mg}^{-1} \text{min}^{-1}$).

NAP removal from seawater samples. Through the adsorption studies, an equilibrium time of 240 min and an adsorption capacity of 33 mg g^{-1} were obtained. The experimental kinetic data showed a better adjustment to the PSO's model, indicating that chemisorption is the mechanism that governs NAP adsorption. The experimental equilibrium data had a better adjustment to Freundlich's model, which suggests the formation of a heterogeneous multilayered surface.

In the study developed by Eeshwarasinghe et al. (2018), PAHs (naphthalene, acenaphene, acenaphene, fluorene and phenanthrene) were removed from wastewater using granular activated carbon (GAC). Batch adsorption and fixed-bed column experiments were conducted to evaluate the efficiency of GAC in the PAHs removal. For the batch adsorption experiments, the kinetic data were better adjusted to the PFO's model, which points out that the main mechanism associated with this process is the physisorption. The experimental data of batch equilibrium adsorption were better described by the Freundlich's model, which suggests heterogeneous adsorption. In dynamic adsorption by fixed-bed column, the curves had a better adjustment to the Thomas's model. The results showed that the batch adsorption and the fixed bed column were able to effectively remove PAHs from wastewater.

Table 3 displays the results obtained for several studies by adjusting the PFO and PSO models to the experimental kinetic data for the adsorption of PAHs from wastewater by different nanoadsorbent materials. In the studies evaluated, the PSO model had a better adjustment to the kinetic experimental data of PAHs adsorption from wastewater, inferring that chemisorption is the main mechanism involved in this process. This model is derived from the Langmuir's kinetic model equation, which states that the adsorptive process is governed by chemical reactions that occur on a homogeneous surface. Generally, the PSO model best represents the kinetic data for most adsorptive systems, as it has the ability to "smooth out" the experimental data, in addition to providing the best correlation for the systems studied, over the entire process time, however, this model is better suited to experimental data in the initial stages of the adsorptive process (Ho and McKay, 1999; Plazinski et al., 2009).

4.3. Adsorption modelling for packed beds

The dynamic modeling of adsorption is very important because it allows the development of models that can help in predicting the mechanisms involved in the adsorptive processes. The most applied mathematical models for fixed-bed adsorption columns are based on the hypotheses of axial dispersion, external mass transfer, intraparticle diffusion and non-linear isotherms (Ruthven, 1984). The main models for studying column adsorption are: Thomas, Bohart-Adams and Yoon-Nelson. Thomas's model is the most used for the study of adsorption columns. However, other alternative models have been developed, aiming at modeling fixed-bed adsorption columns, including the Dual Site Diffusion's model (DualSD), which starts from the principles of the mass conservation law. The main models for fixed-bed

adsorption columns are displayed in Table 4.

Mortazavi et al. (2019) performed the thermal reduction of graphene oxide (GO), followed by chemical bonding to amino-functionalized sand particles (AFSPs) to obtain a nanoadsorbent. The nanoadsorbent obtained was applied to the adsorption of PAHs (NAP and ACE) from wastewater. For batch experiments, a CCD type of experimental design was applied to evaluate the effects of the factors: initial PAH concentration, total dissolved solids (TDS), contact time and adsorbent dosage. The experimental kinetic data had a better adjustment to the PSO and intraparticle diffusion models, while the experimental equilibrium data had a better adjustment to the Langmuir's, Redlich-Peterson's and Dubinin-Radushkevich's models for NAP and for ACE the experimental data had a better adjustment to the Redlich-Peterson's and Freundlich's models. A continuous flow adsorption was also carried out to evaluate the performance of the adsorbent in a fixed-bed, using a mini-column. The experimental data had a better adjustment to the Thomas's model.

Batch systems are important for determining the kinetic and thermodynamic parameters of the process and are generally applied to small volumes of effluents. On the other hand, continuous flow systems are a simple and economical method that can be applied to the processing of large amounts of wastewater.

4.4. Adsorption isotherms

Through the study of the adsorption isotherms it is possible to determine the equilibrium concentration of the adsorbate (C_e) and the concentration of the adsorbate in the adsorbent phase (q_e). The evaluation of the process occurs at constant temperature, and the amount adsorbed by the adsorbent mass depends on the pressure and the final temperature. Other factors, such as the volume of distribution of the pores and the magnitude of the adsorption enthalpy, are obtained through the adsorption isotherms. Favorable isotherms approach a maximum for high concentrations and tend to be linear for low concentrations (Kinniburgh, 1986). The most used adsorption equilibrium models are displayed in Table 5.

Adeola and Forbes (2019) applied in their study graphene wool (GW) for the adsorption of PHEN and PYR from synthetic wastewater. The variables that influenced the adsorptive processes of PAHs are: pH, temperature, TDS of the solution and initial concentration of PAHs. The kinetic experimental adsorption data had a better fit to the PSO model, which suggests that the chemisorption is the predominant mechanism in the adsorption process. The Sips's model (Freundlich - Langmuir) showed a better adjustment to the experimental data for PHEN and PYR. The value of q_{max} by the Langmuir's model for PHEN and PYR was 5 and 20 mg g^{-1} , respectively, and a 99% of reduction was obtained, for all PAHs from wastewater. Thermodynamic studies have shown that the adsorptive processes have an endothermic and spontaneous nature.

Table 6 displays the values of the maximum adsorption capacity (q_{max}) and the values obtained by adjusting the models to the equilibrium experimental data of PAHs adsorption by different nanoadsorbent materials. The Langmuir's and Freundlich's models are the most used to describe the adsorption equilibrium. In most of the studies evaluated, the Freundlich's model showed a better adjustment to the equilibrium data, which indicates that the PAHs adsorption occurs in multilayers with interaction between the adsorbed molecules.

4.5. Adsorption thermodynamics

The values of the Gibbs free energy variation (ΔG°), entropy variation (ΔS°) and enthalpy variation (ΔH°) are calculated through thermodynamic studies, so that, it is possible to understand the characteristics of the adsorptive processes. The processes are considered exothermic when ($\Delta H^\circ < 0$), otherwise the processes are endothermic ($\Delta H^\circ > 0$). It is also possible to determine the spontaneity of the system, so that the adsorptive process has a spontaneous nature when ($\Delta G^\circ < 0$), or not spontaneous nature ($\Delta G^\circ > 0$). The adsorbent has high affinity

Table 3

Parameters of the pseudo-first order and pseudo-second order models adjusted to the adsorption kinetic data obtained under experimental conditions of initial PAH concentration, temperature, pH, stirring speed, contact time and dosage of different nanoadsorbent materials.

PAHs	Nanoadsorbent	Experimental conditions	Pseudo-first-order (PFO)			Pseudo-second-Order (PSO)			References
			q _e (mg g ⁻¹)	k ₁ (min ⁻¹)	R ²	q _e (mg g ⁻¹)	k ₂ (g mg ⁻¹ min ⁻¹)	R ²	
NAP	Functionalized MCM-41	C ₀ : 30 mg L ⁻¹ , 298 K, pH 4, 200 rpm, 20 min, D: 0.02 g.L ⁻¹	41	0.049	0.949	67	0.00124	0.9957	Albayati and Kalash (2020)
ANT	N-Doped Reduced Graphene Oxide (NRGO)	C ₀ : 1 mg.L ⁻¹ , 298 K, pH 7, 150 rpm, 48 h, D: 10 g.L ⁻¹	6.416	0.001	0.956	8.771	6.66 × 10 ⁻⁵	0.876	Song et al. (2021)
NAP	Chitosan beads modified with iron oxide (FeO) and titanium dioxide (TiO ₂) (Ch-FeO/TiO ₂)	C ₀ : 100 ppm, 298 K, pH: 8, 175 rpm, 48 h, D: 3 g.L ⁻¹	19.9	0.0169	0.8885	36.4	0.0011	0.9952	Ruiz et al. (2020)
NAP ACN PHEN	Silica-based organic-inorganic nanohybrid material (NH ₂ -SBA-15)	C ₀ (NAP): 6 mg.L ⁻¹ , C ₀ (ACN): 6 mg.L ⁻¹ , C ₀ (PHN): 4 mg.L ⁻¹ , 298 K, pH 5, 150 rpm, 24 h, D: 3 g.L ⁻¹	NAP: 1.20 ACN: 1.02 PHEN: 0.403	NAP: 0.78 ACN: 2.06 PHEN: 0.361	NAP: 0.942 ACN: 0.837 PHEN: 0.975	NAP: 1.26 ACN: 1.10 PHEN: 0.43	NAP: 1.19 ACN: 2.81 PHEN: 0.46	NAP: 0.975 ACN: 0.914 PHEN: 0.988	Balati et al. (2015)
NAP FLU	ZnO/Ag/GO nanocomposite Hydroxyl functionalized multiwall carbon nanotubes (MWCNT-OH)	C ₀ : 50 mg.L ⁻¹ , 298 K, 20 min, D: 0.25 g.L ⁻¹ C ₀ (NAP): 5 µg L ⁻¹ , C ₀ (FLU): 5 µg L ⁻¹ , 293 K, 5–30 min, D: 10 mg L ⁻¹	NAP: 1.081 FLU: 0.731	NAP: 0.021 FLU: -0.079	NAP: 0.069 FLU: 0.276	NAP: 57.471 FLU: 59.880	NAP: 0.058 FLU: 0.444	NAP: 1.000 FLU: 0.997	Mukweho et al. (2020) Akinpelu et al. (2019)
NAP ACE	Graphene oxide (GO) on the surface of amino-functionalized sand particles	C ₀ (NAP): 400 µg L ⁻¹ , C ₀ (ACE): 400 µg L ⁻¹ , 2 h, D: 8 g L ⁻¹	NAP: 1.7038 ACE: 2.332	NAP: 0.0275 ACE: 0.0275	NAP: 0.9188 ACE: 0.9188	NAP: 2.963 ACE: 3.418	NAP: 0.0204 ACE: 0.0132	NAP: 0.9970 ACE: 0.9953	Mortazavi et al. (2019)
ACE	Modified silicagel	C ₀ (ACE): 3.31 µg L ⁻¹ , 298 K, 350 rpm, 1–5 h, D: 1 mg.L ⁻¹	0.227	0.167	0.983	0.258	0.817	0.959	Hall et al. (2009)
NAP ACE ACN FLU PHEN	Granular Activated Carbon (GAC)	C ₀ (NAP): 6 mg L ⁻¹ , C ₀ (ACE): 6 mg L ⁻¹ , C ₀ (ACN): 6 mg.L ⁻¹ , C ₀ (FLU): 6 mg L ⁻¹ , C ₀ (PHE): 6 mg L ⁻¹ , 297 K, 120 rpm, 24 h, D: 2–50 mg.L ⁻¹	NAP: 13.8 ACE: 14.7 ACN: 15.7 FLU: 13.0 PHEN: 11.8	NAP: 0.0113 ACE: 0.01 ACN: 0.0116 FLU: 0.0085 PHEN: 0.0086	NAP: 0.993 ACE: 0.995 ACN: 0.997 FLU: 0.993 PHEN: 0.994	NAP: 17.3 ACE: 18.5 ACN: 20.5 FLU: 20.5 PHEN: 16.5	NAP: 0.00061 ACE: 0.00053 ACN: 0.0005 FLU: 0.00051 PHEN: 0.0006	NAP: 0.983 ACE: 0.997 ACN: 0.991 FLU: 0.996 PHEN: 0.999	Eshwarasinghe et al. (2018)
PYR BAP	Green synthesized iron oxide nanoparticles (IONPs)	C ₀ (PYR): 100 µg L ⁻¹ , C ₀ (BAP): 1 µg.L ⁻¹ , pH 7, 150 min, D: 90 mg.L ⁻¹	PYR: 0.992 BAP: 0.0094	PYR: 18.9 BAP: 15.7	PYR: 0.96 BAP: 0.887	PYR: 0.96 BAP: 0.0099	PYR: 0.034 BAP: 0.0023	PYR: 0.999 BAP: 0.996	Hassan et al. (2018)
NAP ACE FLU ANT PYR FLT	Granular activated carbon (GAC)	C ₀ (NAP): 5 mg L ⁻¹ , C ₀ (ACE): 20 mg L ⁻¹ , C ₀ (FLU): 5 mg L ⁻¹ , C ₀ (ANT): 20 mg.L ⁻¹ , C ₀ (PYR): 5 mg.L ⁻¹ , C ₀ (FLT): 10 mg.L ⁻¹ , 294 K, pH 7, 400 min, D: 0.6 g.L ⁻¹	NAP: 12.12 ACE: 15.22 FLU: 10.59 ANT: 14.60 PYR: 7.11 FLT: 9.88	NAP: 0.012 ACE: 0.0099 FLU: 0.021 ANT: 0.015 PYR: 0.014 FLT: 0.011	NAP: 0.87 ACE: 0.97 FLU: 0.92 ANT: 0.93 PYR: 0.91 FLT: 0.90	NAP: 15.19 ACE: 20.81 FLU: 12.90 ANT: 15.50 PYR: 12.89 FLT: 18.76	NAP: 1.7 × 10 ⁻⁵ ACE: 3.2 × 10 ⁻⁴ FLU: 5.7 × 10 ⁻⁴ ANT: 5.9 × 10 ⁻⁴ PYR: 3.1 × 10 ⁻⁴ FLT: 1.4 × 10 ⁻⁴	NAP: 0.95 ACE: 0.97 FLU: 0.99 ANT: 0.99 PYR: 0.98 FLT: 0.70	Valderrama et al. (2008)
PHEN PYR	Graphene wool (GW)	C ₀ (PHEN): 50 ng.L ⁻¹ , C ₀ (PYR): 50 ng.L ⁻¹ , 298 K, pH(PHEN) 6.8, pH(PHEN) 6.7, 200 rpm, 24 h, D: 0.5 mg.mL ⁻¹	PHEN: 6.02 PYR: 28.33	PHEN: 1.028 × 10 ⁻³ PYR: 1.29 × 10 ⁻³	PHEN: 0.4227 PYR: 0.5772	PHEN: 28.33 PYR: 41.84	PHEN: 1.43 × 10 ⁻³ PYR: 6.83 × 10 ⁻⁴	PHEN: 0.9998 PYR: 0.9995	Adeola and Forbes (2019)
PHEN ANT	Nanoscale zero-valent iron nanoparticles (NZVIs) (Fe@SiO ₂ @PDA)	C ₀ (PHEN): 0.5 mg.L ⁻¹ , C ₀ (ANP): 0.4 mg.L ⁻¹ , 298 K, pH 7, 200 rpm, 5 min to 12 h, D: 2 g.L ⁻¹	PHEN: 0.089 ANT: 0.035	PHEN: 0.003 ANT: 0.003	PHEN: 0.795 ANT: 0.772	PHEN: 0.194 ANT: 0.367	PHEN: 0.15 ANT: 2.22	PHEN: 0.998 ANT: 0.999	Li et al. (2017)

C₀: Initial concentration of PAHs; D: Adsorbent dosage; q_e: Adsorbate concentration in equilibrium on the adsorbent surface (mg.g⁻¹); k₁: Pseudo-first-order rate constant (min⁻¹); k₂: Pseudo-second-order rate constant (g.mg⁻¹.min⁻¹).

Table 4
Models for fixed-bed adsorption columns.

Models	Equation
Thomas (1944)	$\ln\left(\frac{C_0}{C_t} - 1\right) = \frac{K_T q_0 m}{Q} - K_T C_0 t \quad (5)$
Bohart-Adams (1920)	$\ln\left(\frac{C_t}{C_0}\right) = K_{BA} C_0 t - \frac{K_{BA} N_0 Z}{V} \quad (6)$
Yoon-Nelson (1984)	$\ln\left(\frac{C_t}{C_0 - C_t}\right) = K_{YN} t - \tau K_{YN} \quad (7)$
Dual Site Diffusion (DualSD) (2020) Andrade et al.	$\frac{\partial C}{\partial t} = D_a \frac{\partial^2 C}{\partial z^2} - u_0 \frac{\partial C}{\partial z} - \frac{\rho_B}{\epsilon} \frac{\partial q}{\partial t} \quad (8)$

C_0 : initial concentration of contaminant (mg L^{-1}), K_T : constant of Thomas's model ($\text{L min}^{-1} \text{mg}^{-1}$), C_t is the concentration of effluent obtained at time (mg L^{-1}), m : mass of the adsorbent in the column (g), Q : flow rate (mL.min^{-1}), q_0 : capacity of adsorption obtained from Thomas's model (mg g^{-1}), K_{BA} : Bohart-Adams kinetic rate constant ($\text{L min}^{-1} \text{mg}^{-1}$), N_0 : capacity of adsorption of the adsorbent obtained from Bohart-Adams's model (mg.g^{-1}), Z : height (or length) of the bed (cm), V : linear speed (velocity) (cm.min^{-1}), K_{YN} : Yoon-Nelson proportional constant (min^{-1}) and τ is the time when $C_t = 0.5 C_0$, C : concentration of pollutant in the liquid phase (mmol L^{-1}), q : amount of pollutant at the adsorbent (mmol g^{-1}), D_a : axial dispersion coefficient ($\text{cm}^2 \text{min}^{-1}$), u_0 : interstitial velocity (cm min^{-1}), ρ_B : fixed-bed density (g L^{-1}) and ϵ : void fraction.

Table 5
Main adsorption equilibrium models.

Models	Equation
Langmuir (1918)	$q_e = \frac{q_{max} K_L C_e}{1 + K_L C_e} \quad (9)$
Freundlich (1906)	$q_e = K_F C_e^{\frac{1}{n}} \quad (10)$

q_e : adsorption equilibrium capacity (mg g^{-1}), C_e : equilibrium concentration of adsorbate (mg L^{-1}), q_{max} : maximum adsorption capacity (mg g^{-1}), K_L : Langmuir's equilibrium constant associated with the affinity of the sites (L mg^{-1}), K_F : Freundlich's constant [$(\text{mg g}^{-1})(\text{L mg}^{-1})^{1/n}$] and n is the empirical constant associated with the adsorption intensity.

with adsorbate when ($\Delta S^\circ > 0$) or low affinity when ($\Delta S^\circ < 0$). From the magnitude of these parameters, it is also possible to determine whether the adsorption mechanism is governed by chemisorption or physisorption.

[Sharma et al. \(2017\)](#) performed the synthesis of superparamagnetic nanocomposites carbon/ZnFe₂O₄ (C/ZnFe₂O₄) using the reflux method. The nanomaterial obtained was characterized by the techniques of FTIR, XRD, VSM, BET, FESEM, HRTEM and EDX. C/ZnFe₂O₄ was used in the adsorption of NAP and 2-naphthol from wastewater, in a batch adsorption process. The kinetic and equilibrium experimental data had a better adjustment to the PFO and Langmuir's models, respectively. Through the thermodynamic adsorption, the parameters ΔH° , ΔS° and ΔG° were determined, which influences the nature of the adsorption. The results indicated that the adsorptive process had a spontaneous nature ($\Delta G^\circ < 0$), in addition to presenting high affinity for adsorbate ($\Delta S^\circ > 0$). The ΔH° value was positive ($\Delta H^\circ > 0$), so the process is endothermic, which indicates that the adsorption was governed, mainly, by the physisorption mechanism, which was also confirmed by the adjustment of the equilibrium data to the Langmuir's model.

[Yang et al. \(2013\)](#) synthesized rGO/FeO•Fe₂O₃ nanocomposites, in which rGO stands for the reduced form of GO, aiming at their application in the adsorption of contaminants 1-naphthylamine, 1-naphthol and NAP, from synthetic wastewater. The experimental equilibrium data had a better adjustment to Freundlich's model, for all pollutants, indicating the presence of heterogeneous adsorption sites. The thermodynamic

studies of NAP adsorption showed that the calculation of the parameters ΔH° , ΔS° and ΔG° , indicated that the adsorptive process has a spontaneous nature ($\Delta G^\circ < 0$), endothermic nature ($\Delta H^\circ > 0$) and a high affinity of adsorbate (NAP) for the adsorbent (rGO/FeO•Fe₂O₃) ($\Delta S^\circ > 0$).

[Table 7](#) displays the thermodynamic parameters and experimental data from several PAHs adsorption studies using different nano-adsorbent materials. The results showed that most PAHs adsorption processes are endothermic, as they present positive values of enthalpy variation (ΔH°), which vary from -51.2 – $40.98 \text{ kJ mol}^{-1}$, depending on the system. The results also showed that most of the processes are spontaneous, as they present negative values of variation of Gibbs Free Energy (ΔG°). [Table 7](#) also shows that in most studies the values of entropy variation (ΔS°) are positive, ranging from -164 – $161.21 \text{ J mol}^{-1} \cdot \text{K}^{-1}$, according to the system. The PAHs evaluated have a high affinity for the adsorbents, according to the results presented in the evaluated articles.

5. Nanomaterial-based adsorbents

According to the recommendations of IUPAC (2012), nanomaterials can be defined as materials whose particles in any form have dimensions that vary in a nanoscale of 1–100 nm ([Vert et al., 2012](#)). The most common types of nanomaterials are: nanofilaments, nanopowders, nanotubes, nanowires, nanocables, nanofilms and nanoblocks. Different physical, chemical or mechanical mechanisms can be applied for the preparation of nanomaterials, according to the desired characteristics ([Zhang, 2018](#)).

The relationship between surface area and volume is one of the factors responsible for the characteristics of a given nanomaterial. The main physical properties are melting point and optical adsorption vary depending on the size and shape of the nanomaterials ([Asha and Narain, 2020](#)). Nanomaterials can be characterized in terms of shape and dimensionality, so that they can be classified into four categories ([Pokropivny and Skorokhod, 2007](#)), as illustrated in [Fig. 3](#):

- Zero-dimensional (0D): Nanoparticles, molecules, clusters, fullerenes, rings, particles, grains, powders, schwartzons, metcarbs and thoroids;
- One-dimensional (1D): Nanotubes (CNT), nanowires, nanofibers, springs, needles and pillars;
- Two-dimensional (2D): Nanofilms (Graphene), nanolayers;
- Three-dimensional (3D): Nanocrystalline structure, powder skeletons and skeletons of fiber.

Particle size is a very important parameter, as its decrease can directly affect the particle's interaction in the chemical reactions, since the decrease of the particle size can increase the number of pending (or exposed) bonds in the reaction environment. On the other hand, the decrease in particle size can generate an exponential increase in the reaction speed, as well as a decrease in the reaction temperature. Nanomaterials have some important enhanced chemical properties, such as a greater number of reactive sites, high hydrophilicity and the possibility of functionalization ([Mercier et al., 2002](#)).

The mechanical properties of nanomaterials vary according to the type of base material, environment and external loads. To carry out an in-depth analysis of the mechanical properties, some factors must be taken into account, such as, the surface structure, porosity, functionalization, preparation methods and chemical treatments. Metallic nanomaterials have as main mechanical properties: resistance, plasticity, hardness, tenacity, fragility, elasticity, ductility, stiffness and yield stress. Inorganic non-metallic materials, on the other hand, are mostly fragile, and organic materials do not have properties such as, rigidity and fragility, most of which are flexible ([Reghunadhan et al., 2018](#); [Wu et al., 2020](#)).

The surface reactivity of nanomaterials is attributed to their chemical, physical and mechanical properties. Their high surface reactivity

Table 6
Models of adsorption isotherms for the removal of PAHs by different nanoadsorbent materials.

PAHs	Nanoadsorbent	Experimental conditions	Isotherm models	q _{max} (mg.g ⁻¹)	Additional information	References
NAP ANT PYR	Reduced graphene oxides (rGOs)	C ₀ (NAP): 0.1 mmol L ⁻¹ , C ₀ (ANT): 0.1 mmol L ⁻¹ , C ₀ (PYR): 0.1 mmol L ⁻¹ , 298 K, pH: 6.5	L F	NAP: 766.59 ANT: 80.92 PYR: 198.003	L (NAP): K _L = 0.0223, R ² = 0.966 L (ANT): K _L = 0.411, R ² = 0.963 L (PYR): K _L = 0.343, R ² = 0.976 F (NAP): K _F = 15.92, 1/n = 0.928, R ² = 0.998 F (ANT): K _F = 247.17, 1/n = 0.312, R ² = 0.978 F (PYR): K _F = 369.06, 1/n = 0.298, R ² = 0.998	Sun et al. (2013)
NAP	ZnO/Ag/GO nanocomposite	C ₀ : 50 mg.L ⁻¹ , 298 K, 20 min, D: 0.25 g.L ⁻¹	L F	500	L: K _L = 0.0247, R ² = 0.67 F: K _F = 8.166, 1/n = 0.13, R ² = 0.95	Mukwevho et al. (2020)
NAP FLU	Hydroxyl functionalized multiwall carbon nanotubes (MWCNT-OH)	C ₀ (NAP): 5 µg.L ⁻¹ , C ₀ (FLU): 5 µg.L ⁻¹ , 293 K, 5–30 min, D: 10 mg.L ⁻¹	L F	NAP: 57.401 FLU: 61.235	L (NAP): K _L = 277.78, R ² = 0.9703 L (FLU): K _L = 1428.6, R ² = 0.9517 F (NAP): K _F = 177.73, 1/n = 0.585, R ² = 0.9614 F (FLU): K _F = 330.04, 1/n = 0.373, R ² = 0.7767	Akinpelu et al. (2019)
NAP	Graphene (G) and Graphene oxide (GO)	C ₀ (NAP): 5 mg.L ⁻¹ , 296 K, pH 5, 24 h	F	–	F (G): K _F = 14.17, n = 0.47, R ² = 0.97 F (GO): K _F = 0.93, n = 0.40, R ² = 0.99	Pei et al. (2013)
NAP	Reduced graphene oxide/iron oxide (GO/FeO•Fe ₂ O ₃)	C ₀ (NAP): 0.156 mmol.L ⁻¹ , 283.15 K, pH 7, 48 h, D: 0.1 g.L ⁻¹	L F	337.088	L: K _L = 2.42 × 10 ⁻³ , R ² = 0.981 F: K _F = 0.0223, n = 0.65, R ² = 0.981	Yang et al. (2013)
PYR BAP	Green synthesized iron oxide nanoparticles (IONPs)	C ₀ (PYR): 100 µg.L ⁻¹ , C ₀ (BAP): 1 µg.L ⁻¹ , pH 7, 150 min, D: 90 mg.L ⁻¹	L F	0.895	L (PYR): K _L = 1.62 × 10 ⁻⁴ , R ² = 0.905 L (BAP): K _L = 3.37 × 10 ⁻⁴ , R ² = 0.981 F (PYR): K _F = 6.3 × 10 ⁻⁴ , n = 3.14, R ² = 0.895 F (BAP): K _F = 0.31 × 10 ⁻⁴ , n = 3.56, R ² = 0.97	Hassan et al. (2018)
NAP ACE	Graphene oxide (GO) on the surface of amino-functionalized sand particles	C ₀ (NAP): 400 µg.L ⁻¹ , C ₀ (ACE): 800 µg.L ⁻¹ , 2 h, D: 10 g.L ⁻¹	L F	NAP: 6.555 × 10 ⁻³ ACE: 0.0178	L (NAP): K _L = 1.776, R ² = 0.999 L (ACE): K _L = 1.7899, R ² = 0.965 F (NAP): K _F = 5.616, n = 1.541, R ² = 0.9963 F (ACE): K _F = 16.373, n = 1.3031, R ² = 0.999	Mortazavi et al. (2019)
PHEN PYR	Graphene wool (GW)	C ₀ : 1–5 mg.L ⁻¹ , 298 K, pH _(PHEN) : 6.8, pH _(PYR) : 6.7, 200 rpm, 24 h, D: 0.667 g.L ⁻¹	L F	PHEN: 5.0 PYR: 20.0	L (PHEN): K _L = 181.8, R ² = 0.9793 L (PYR): K _L = 6.85, R ² = 0.9635 F (PHEN): K _F = 16.2, n = 0.6218, R ² = 0.9906 F (PYR): K _F = 114.4, n = 0.9665, R ² = 0.9685	Adeola and Forbes (2019)
NAP	Chitosan beads modified with iron oxide (FeO) and titanium dioxide (TiO ₂) (Ch-FeO/ TiO ₂)	C ₀ : 80 ppm, 298 K, pH: 8, 175 rpm, 48 h, D: 3 g.L ⁻¹	L F	149.3	L: K _L = 0.47, R ² = 0.9303 F: K _F = 52.57, n = 1.12, R ² = 0.9979	Ruiz et al. (2020)
ANT	N-Doped Reduced Graphene Oxide (NRGO)	C ₀ : 1 mg.L ⁻¹ , 298 K, pH 7, 150 rpm, 48 h, D: 10 g.L ⁻¹	L F	2.811	L: K _L = 46.195, R ² = 0.772 F: K _F = 380.277, n = 0.873, R ² = 0.983	Song et al. (2021)

C₀: Initial concentration of PAHs; D: Adsorbent dosage; L: Langmuir model; F: Freundlich model; K_L: Langmuir equilibrium constant related to the affinity of the binding sites (L.mg⁻¹); K_F: Freundlich constant related to the adsorption capacity [(mg.g⁻¹).(L.mg⁻¹)^{1/n}]; n: Empirical constant related to the intensity of adsorption (dimensionless); q_{max}: Maximum adsorption capacity (mg.g⁻¹).

Table 7
Thermodynamic parameters for the removal of PAHs by different nanoadsorbent materials.

PAHs	Nanoadsorbent materials	T (K)	ΔG° (kJ mol ⁻¹)		ΔH° (kJ mol ⁻¹)		ΔS° (J mol ⁻¹ K ⁻¹)		References
			PYR	BAP	PYR	BAP	PYR	BAP	
PYR BAP	Green synthesized iron oxide nanoparticles (IONPs)	293	PYR	BAP	PYR	BAP	PYR	BAP	Hassan et al. (2018)
		303	-1.7×10^{-3}	-2.17×10^{-3}	-17.2×10^{-3}	-22.13×10^{-3}	-52.68	-67.07	
		313	-1.4×10^{-3}	-1.78×10^{-3}					
		323	-0.95×10^{-3}	-1.10×10^{-3}					
NAP	Functionalized MCM-41	298	-7.831		-23.004		-50.273	Albayati and Kalash (2020)	
		308	-7.393						
		318	-6.8456						
NAP	Reduced graphene oxide/iron oxide (GO/FeO•Fe ₂ O ₃)	283	-4.31		40.98		161.21	Yang et al. (2013)	
		303	-8.26						
		323	-10.70						
NAP	Carbon/ZnFe ₂ O ₄	303	-2.16		11.51		45.12	Sharma et al. (2017)	
		313	-2.61						
		323	-3.07						
		333	-3.32						
		343	-3.97						
PHEN	Orange Rind Activated Carbon (ORAC)	293	10.40		20.47		0.1138	Gupta and Singh (2018)	
		303	12.14						
		313	12.61						
		323	14.04						
PHEN ANT	Nanoscale zero-valent iron nanoparticles (NZVIs) (Fe@SiO ₂ @PDA)	298	PHEN	ANT	PHEN	ANT	PHEN	ANT	Li et al. (2017)
		303	-2.40	-5.15	-51.2	-17.1	-164.0	40.0	
		308	-1.55	-4.94					
NAP ANT PYR	Rice straw (RS) and Sugarcane bagasse (SB)	288	RS SB		RS SB		RS SB	Younis et al. (2014)	
			NAP: 6.08 5.50		NAP: 20.10 21.32		NAP: 48.9 54.9		
			ANT: 7.36 6.22		ANT: 14.66 16.94		ANT: 25.6 37.1		
			PYR: 7.39 6.52		PYR: 10.48 19.07		PYR: 10.9 43.2		

Thermodynamic parameters can be expressed by equations: $\Delta G^\circ = -R T \ln K_C$ and $\Delta G^\circ = \Delta H^\circ - T \Delta S^\circ$, where K_C : constant of chemical equilibrium, R : ideal gas constant (8.314 J mol⁻¹ K⁻¹) and T : temperature (K).

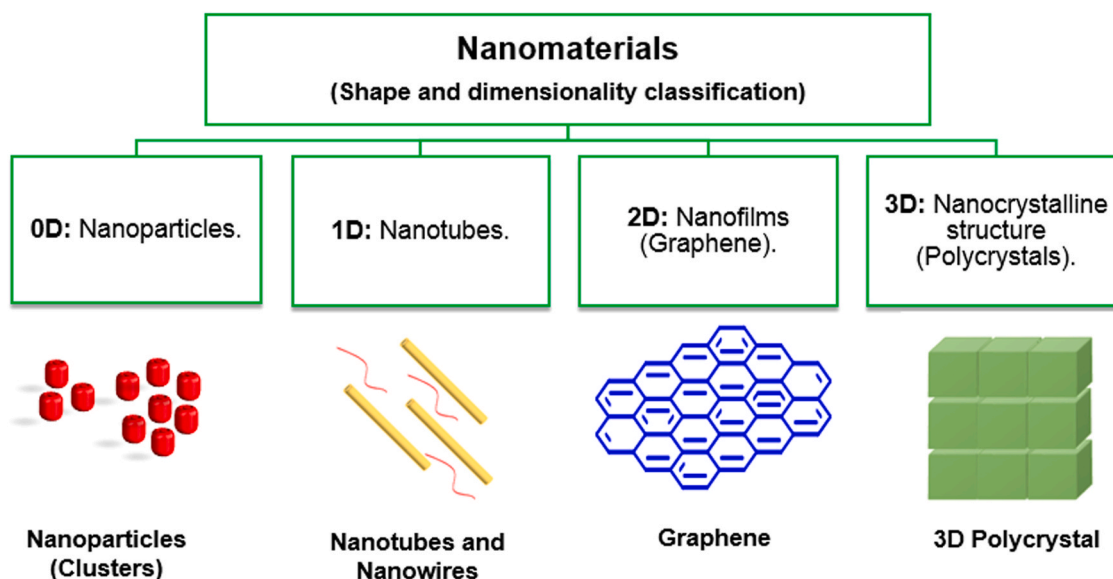


Fig. 3. Classification of nanomaterials, based on shape and dimension, in zero-dimensional (0D), one-dimensional (1D), two-dimensional (2D) and three-dimensional (3D).

enables the nanometric crystals to aggregate into micrometric particles. Some nanomaterials have unique adsorptive properties that are attributed to the differences in reactive surface sites and also to regions of disorder on the surface (Chakravarty and Dash, 2013).

Carbon-based nanomaterials can be applied in wastewater treatment processes to remove polluting compounds. Factors such as the presence of functional groups, pore size and volume, degree of polarity, among others, directly influences the remediation processes. The analysis of the physical-chemical characteristics of adsorbents based on nanomaterials influences the performance of the adsorbent in the adsorption and

desorption processes. The evaluation of the performance of the adsorbents is carried out by means of adsorption tests under stationary and dynamic conditions (Chakravarty and Dash, 2013; Saleh et al., 2019).

Mukweho et al. (2020) performed the synthesis of the ZnO/Ag/GO nanocomposite. The nanomaterial was applied for the adsorption and photodegradation of NAP from synthetic wastewater by visible light. The adsorbent obtained was characterized by the techniques of XRD, UV-vis, FTIR, XPS, SEM and TEM, through which it was possible to determine the chemical, structural and morphological characteristics of the nanomaterial. The XRD analysis confirmed the hexagonal structure

of the nanoparticles, indicating that the introduction of Ag and GO did not alter the hexagonal structure of ZnO. Then, the nanomaterial was applied in adsorption and later in the photodegradation of NAP. The kinetic and equilibrium experimental data had a better adjustment to the PSO and Freundlich's model, respectively. An adsorption capacity of 500 mg.g^{-1} was obtained and 80% of NAP reduction was achieved in a contact time of 20 min. The efficiency of removal of NAP improved after the application of the photodegradation process, obtaining 92% of reduction in 50 min.

Zhang et al. (2019) reported the synthesis of three carbon-based magnetic nanomaterials (CNMs), MMWCNTs, MSWCNT and MGNS, which were applied for PHEN removal from wastewater. The results obtained through the characterizations by TEM, FTIR and XRD, indicated that the CNMs were coated with iron oxide nanoparticles. The determination of magnetism showed that there was the formation of magnetic nanoparticles. The PSO model had a better adjustment to the adsorption kinetic data, while the Dubinin-Astakhov's model had a better adjustment to the adsorption equilibrium data. The thermodynamic parameters (ΔG° , ΔH° and ΔS°) are negative, which indicates that the adsorptive process of PHEN by the synthesized CNMs is spontaneous, exothermic and with reduced entropy.

Graphene-based materials have gained prominence in the remediation processes of organic, inorganic and gaseous contaminants, due to their high surface area and relatively low production cost. Given these advantages, graphene-based adsorbents can be applied in the PAHs adsorption processes from wastewater. Huang et al. (2019) reported the PHEN adsorption by magnetic graphene oxide (MGO), chemically reduced magnetic graphene (MCRG) and reduced graphene by magnetic annealing (MARG), from synthetic wastewater. The factors pH, heavy metal ions and natural organic matter concentrations, had their effect evaluated. MCRG showed a greater adsorption capacity for PHEN, due to the higher surface area and pore volume, obtained for MCRG adsorbent. The π - π interaction was the dominant mechanism in the MCRG adsorption process. Dubinin-Astakhov's model had a better adjustment to the experimental equilibrium data.

Huang et al. (2018) prepared rGO/polyHIPEs emulsions by using 2-ethylhexyl acrylate and ethylene glycol dimethacrylate. The adsorbent materials obtained were applied for PAHs adsorption from wastewater. SEM analysis showed a superficial open cell morphology, which contributes to good permeability and rapid mass transfer. The surface area of the materials was determined by the BET method, which indicated that the specific surface area increased when the amount of rGO increased. The adsorption isotherms indicated that the adsorbents showed a higher adsorption capacity and good cycle stability for PAHs. The predominant mechanism of adsorption was the π - π and hydrophobic interaction. After the adsorption process with rGO/polyHIPEs, the levels of PAHs present in the water decreased, falling below the standard value established by the European Food Safety Authority (EFSA).

5.1. Graphene-based nanomaterials: conventional chemistry

The application of graphene-based materials as adsorbents to remove contaminants from the environment has gained prominence in the current context. Graphene-based materials have unique physicochemical properties, such as high specific area, thermal conductivity, electron mobility and mechanical strength, which makes graphene an ideal material for applications in adsorption processes of organic components in the oil industry (Perreault et al., 2015).

Graphene-based materials present a 2D layer of sp^2 -hybridized carbon atoms, forming a hexagonal structure, similar to an ordered honeycomb. It often exhibits excellent thermal and electrical conductivity, and mechanical strength (Stankovich et al., 2006). Graphene has gained notoriety since 2004, when it was first isolated from graphite by the mechanical exfoliation method, whose methodology was described by Novoselov et al. (2004). Since then, its properties have been explored aiming its application in different processes, such as adsorption,

separation and photocatalysis. Therefore, some studies have been developed with a main focus on the properties of graphene for its application in the separation of toxic compounds present in oily waters of the petroleum industry.

Alghunaimi et al. (2019) synthesized a material based on graphene grafted with 9-octadecenoic acid, the material obtained was applied for the remediation of organic pollutants from oily water. Graphene was synthesized from graphite through a chemical treatment process, then it was grafted with 9-octadecenoic acid, which is used as a linker agent, forming the 9-octadecenoic acid grafted graphene (OG). Then, an emulsion polymerization of styrene was carried out, in order to obtain a hydrophobic material, POG. FTIR and SEM analyzes confirmed the presence of graphene in the structure of the synthesized materials. The performance of POG composites in the separation of organic pollutants (hexane, heptane, nonane, decane and hexadecane) from water was evaluated. The results indicated that the greater the proportion of graphene grafted with 9-octadecenoic acid, the greater the absorption efficiency of the composite and the faster the adsorption rate of the organic components. A regeneration study of the composite was also carried out, which indicated that the adsorption rate remained constant. The study pointed out that the POG has potential application for the remediation of organic pollutants from effluents of the oil industry, among which PAHs can be included.

Graphene oxide (GO) has a monolayer, which is obtained by treating graphene with strong oxidants, containing in its structure functional groups, such as hydroxyl, carboxyl, carbonyl and epoxy (Zhang et al., 2016). The preparation of graphene oxide (GO) was carried out for the first time by Brodie (1859), who subjected Ceylon graphite to a treatment with an oxidation mixture composed of potassium chlorate and fuming nitric acid. After the Brodie's report in 1859, other procedures were proposed for the formulation of graphene oxide, in which, for the most part, they use mixtures with strong oxidizers (Hummer and Offeman, 1958).

Hummer's method is one of the most used methods by researchers for the production of GO, being introduced by Hummer and Offeman (1958). According to this method, the following reagents are used for the oxidation of graphene: 100 g of graphite powder, 50 g of NaNO_3 , 2.3 L of H_2SO_4 and 300 g of KMnO_4 . One of the advantages of the Hummer's method is that the oxidative process takes a few hours to produce a high amount of GO, in addition to producing a greater amount of oxygen when compared to the Brodie's method. However, one of the main limitations of the Hummer's method is related to the emission of toxic gases, such as NO_2 , N_2O_4 and explosive gases, such as ClO_2 . In addition, the presence of residual ions, Na^+ and NO_3^- , generated due to the use of NaNO_3 as a reagent, can be difficult to remove from the effluents (Chen et al., 2013; Chua and Pumera, 2014).

Some studies have been developed aiming to propose modifications to the Hummer's method in order to minimize the toxic effects attributed to the conventional method. Alkhouzaam et al. (2020) performed the synthesis of GO nanoparticles by the modified Hummer's method, varying operational conditions, such as temperature, reagent stoichiometry and oxidation time. The synthesis of the GO was carried out in two stages: in the first stage, the oxidation of graphite in the GO was carried out; in the second stage, the material was washed, aiming at the elimination of impurities, such as acids, manganese salts, among others. The Hummer's method was modified by varying the reaction temperature, time and reagent stoichiometry, in a NaNO_3 free reaction medium. The obtained materials were characterized by the techniques of SEM, TEM, XPS, FTIR, Raman spectroscopy and TGA. The results of the FTIR spectra indicated the presence of oxygen related bands (ORB), which confirmed the oxidation of graphite. The results of the TGA indicated that the thermal decomposition of the GO depended on the elementary compositions, so that the GO with low oxygen content had high thermal stability and vice versa.

In a study developed by Fadillah et al. (2019), modifications to the Hummer's method for the GO synthesis were proposed. Fadillah et al.

(2019) performed the synthesis of a graphene oxide/alginate (GO/Alg) composite aiming at its potential application for the remediation of dyes from wastewater, through the combination of electrochemical and adsorption techniques. GO was synthesized by the modified Hummer's method using powdered graphite, then the alginate was incorporated into the GO, using CaCl_2 as a crosslinking agent, thus forming the GO/Alg beads. The results of the XRD and FTIR characterizations indicated that GO was successfully synthesized by the modified Hummer's method. The XRD and FTIR analyses, respectively, indicated the characteristic peak of GO and the presence of functional groups C-OH, which indicates that the graphite was effectively oxidized, forming the graphite oxide. The results also indicated that the combination of electrochemical and adsorption techniques were efficient for the remediation of methylene blue (MB) from wastewater.

The methodologies proposed by Alkhouzaam et al. (2020) and Fadillah et al. (2019) for the synthesis of GO, through the modified Hummer's method, are promising methods for the efficient synthesis of GO, contributing to minimize the generation of toxic effluents due to the use of chemical reagents, such as NaNO_3 . The results indicated that the synthesized materials are promising for the remediation of organic pollutants, such as PAHs, from wastewater.

The presence of petrogenic PAHs in the aquatic environment can cause harmful damage to marine biota, due to its toxic and polluting potential, the application of graphene-based adsorbents can decrease the concentration of these contaminants in the marine environment, due to the excellent adsorptive properties of graphene. Álvarez et al. (2021) carried out a study to evaluate the adsorption of petrogenic PAHs from the aquatic environment by applying GO, synthesized by conventional Hummer's method. The materials obtained were characterized by TEM and AFM techniques. Through TEM analysis, it was observed that the maximum platelet length was approximately 13 μm , while through AFM analysis showed a thickness of 0.612 ± 0.176 nm for the GO platelets. The adsorption results indicated a high GO adsorption capacity for BaP, so that, for a initial concentration of $100 \mu\text{g L}^{-1}$, a 98% of reduction was obtained after 40 h. For the other fractions of PAHs, there was a 95.7% of reduction for PHEN, 84.4% for FLU and 51.5% for ACE, after 40 h.

A new type of functionalized graphene oxide, produced by mixing GO with brilliant blue (BB) was proposed by Zhang et al. (2013). GO was synthesized by the modified Hummer's method, and then BB was incorporated into GO, forming a new functional composite BBGO. SEM, AFM and FTIR analyzes indicated that the BBGO composite was successfully obtained, indicating the presence of GO in its structure. BBGO was applied as an adsorbent for the removal of two types of PAHs (anthracenemethanol (AC) and FLT) from a synthetic effluent. The adsorptive experiments were carried out in batch, after the adsorptive process, the AC/BBGO and FLT/BBGO complexes were removed from the system through a coagulation-flocculation process at 60°C and pH 3.0. The adsorption results indicated high adsorption capacity for AC and FLT, a 72% of reduction for AC was obtained after 11 days and a 93.2% of reduction for FLT was obtained after 1.4 h (100 min).

The adsorptive studies carried out by Álvarez et al. (2021) and Zhang et al. (2013) indicated that graphene-based adsorbents are efficient for the removal of PAHs from wastewater, which can be proven by the high adsorption capacities obtained by the studies. The BBGO nanocomposite synthesized by Zhang et al. (2013) demonstrated to be quite promising for the remediation of FLT from effluents.

One of the most important characteristics of GO is that it can be reduced by the reaction of GO with a reducing agent, thus generating GO in its reduced form (rGO). rGO has attracted the attention for its large-scale applications, due to its low production cost. For the reduction of graphene oxide, some methods have been studied, such as thermal reduction, chemical reduction through reducing agents and photoreduction (Pei and Cheng, 2012; Chen and Huang, 2020).

By reducing the GO, the structure and properties of pure graphene are partially restored, but the carbon plane structure remains altered, due to the incomplete removal of the functional groups with oxygen. The

GO reduction aims to eliminate the epoxy and hydroxyl groups, however, the carboxyl, carbonyl and ester groups are still present at the edges and in some defective areas. The rGO, due to modifications of its structure and properties, has an ability to interact with the analyte through π - π or by hydrophobic interactions, which gives it a high affinity for aromatic compounds, such as PAHs (Pei and Cheng, 2012; Gomis et al., 2020). Fig. 4 illustrates the synthesis of graphene from graphite and chemical reduction of GO.

The reduction of graphene oxide can cause changes in its chemical structure, thus generating carbon vacancies, besides that, the presence of residual functional groups in the rGO structure can also cause changes in the mechanical and electronic properties. The process of chemical reduction of the GO can contribute to the reduction of the surface area and electrical conductivity of the material, while the process of thermal reduction can change the structure and the mechanical resistance of the rGO, thus generating a substantial decrease in the mass of the GO (Bagri et al., 2010; Chen and Huang, 2020).

Song et al. (2021) performed the synthesis of rGO doped with nitrogen (NRGO) using the hydrothermal method. The material obtained was used as an adsorbent for the removal of ANT and 2-MAQ, from synthetic wastewater. Through the FTIR analysis, the presence of the functional groups of GO, rGO and NRGO was observed. SEM analysis showed that the degree of aggregation of the NRGO layers is lower than the degree of aggregation of the rGO, which indicates that the introduction of nitrogen into the structure of the rGO reduced the folding of the crushed leaves after the process of thermal reduction, however, it did not destroy the structure of graphene. The equilibrium experimental data were better adjusted to Freundlich's model and the kinetics experimental data were better adjusted to PFO model for ANT and PSO for 2-MAQ. The adsorption capacity of NRGO was 5.77 and 9.29 mg g^{-1} for ANT and 2-MAQ, respectively. The adsorbent remained efficient after the third cycle of use, according to the regeneration study.

Therefore, the study by Song et al. (2021) showed that the reduction of GO, followed by the introduction of nitrogen in its structure, can contribute to improve the properties of GO and increase the adsorption capacity of hydrophobic substances, such as PAHs.

5.2. Adsorption by green graphene-based nanomaterials

Adsorption is one of the most widely used methods for the remediation of pollutants, due to the low cost and high efficiency of contaminant recovery, such as PAHs. The term 'green adsorption' has been widely used to refer to adsorptive processes that use environmentally friendly methods to produce adsorbents from natural, biodegradable and non-toxic sources. Green adsorbents are produced, in general, using agricultural residues or materials that can work at room temperature or in sunlight, thus reducing the process costs (Rani and Shanker, 2018).

Green nanotechnology is used for the production of green adsorbents, aiming to minimize the toxic effects caused by the use of chemical reagents, thus optimizing the synthesis processes of nanomaterials, for the production of adsorbents with pore size and morphology of interest for its application in adsorptive processes. For the synthesis of green nanomaterials, natural agents are used, such as plant extracts, biodegradable materials and microorganisms. Some factors, such as concentration of the extracts, reaction time, precursor agents and pH, influence the synthesis processes of these green materials, as they directly influence the final features of the product (Mahmoud, 2020).

The synthesis processes of nanomaterials, whether by conventional or green chemistry, involve three factors: capping agent, reducing agent and solvent. In processes involving green chemistry, capping agents and reducing agents, in general, are non-toxic and less polluting, whereas the solvents are of natural origin. Capping agents are used to stabilize the nanoparticles, control the morphology and protect the aggregation surface, some capping agents used in green synthesis are polysaccharides and biomolecules, due to their high biocompatibilities and low toxicity. Reducing agents are used in chemical reduction processes,

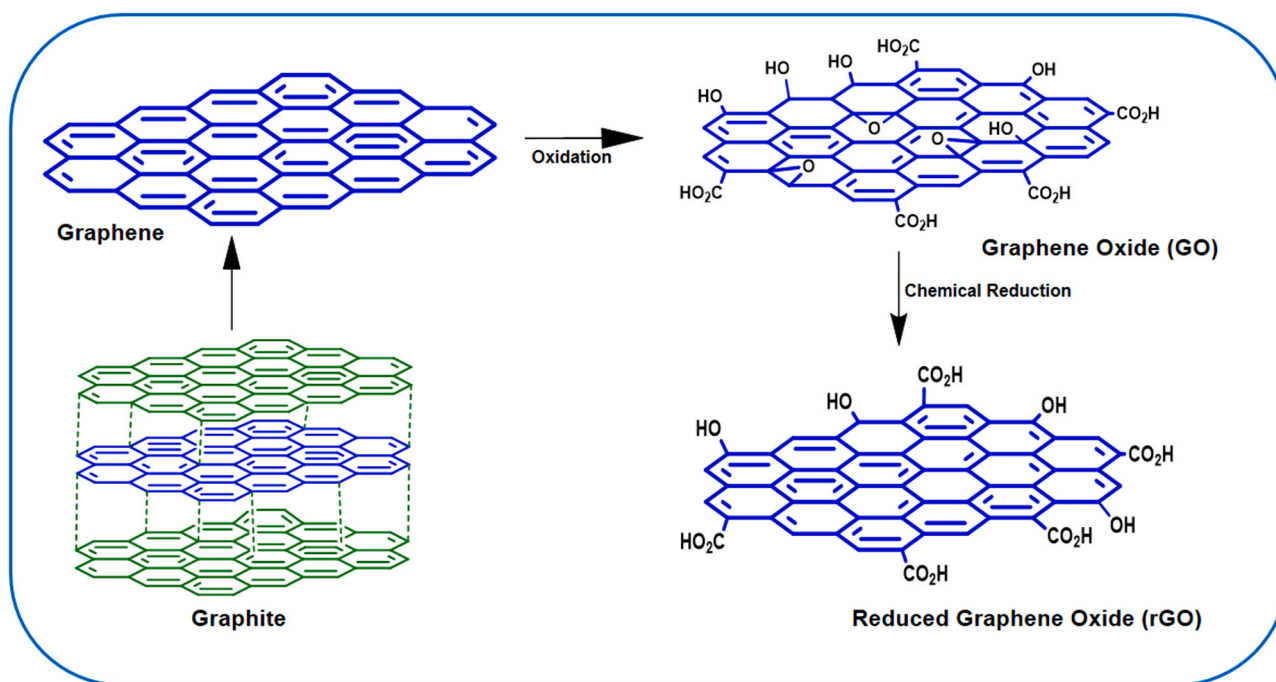


Fig. 4. Synthesis of graphene from graphite and chemical reduction of GO.

polysaccharides, such as β -D-glucose, peptides and proteins can also be used as green reducing agents. Solvents are widely used for the dissolution of precursors, assisting in heat transfer and dispersion of nanoparticles, water is one of the most used solvents because it is environmentally friendly, non-toxicity and non-flammability. Other alternative solvents that have been applied in green synthesis processes are supercritical fluids, supercritical carbon dioxide and ionic liquids (Duan et al., 2015).

The conventional synthesis of graphene-based nanomaterials by the Hummer's method involves the use of chemical reagents harmful to the environment, in this context, some studies have reported the development of green methodologies for the synthesis of these nanomaterials through the use of natural agents, such as plants extracts and biodegradable waste. Table 8 summarizes the sources and methodologies used for the green synthesis of graphene-based nanomaterials. Fig. 5 shows a schematic diagram of the main types of green reducing agents used for

the synthesis of reduced GO.

Tewatia et al. (2020) reported the reduction of GO through the use of a green reducing agent, ascorbic acid, also known as vitamin C. The GO was synthesized by modified Hummer's method, in which NaNO_3 were removed with an increase in the amount of KMnO_4 . To reduce the GO, 5 g of ascorbic acid were added to the aqueous solution with a concentration of 5 g L^{-1} of GO, the solution was stirred at 600 rpm at a constant temperature of 60°C . The results of the FTIR analyzes showed that the functional groups were removed after the chemical reduction process. The XRD analysis showed the presence of a wider peak after the reduction of the GO, which indicates that there was the removal of the functional oxygen group and the restoration of the $\text{C}=\text{C}$ bonds. However, due to the peak width, it was concluded that removal of functional groups containing oxygen was incomplete, in addition, the presence of intercalated H_2O molecules was detected.

Hou et al. (2017) performed the reduction of GO through the use of

Table 8

Summary of sources and methodologies used for the green synthesis of graphene-based nanomaterials.

Nanomaterials	Methodology	Morphology	Characterizations	Other informations	References
GO and rGO	Modified Hummer's method and reduction by Ascorbic acid (vitamin C).	–	XRD, UV–visible spectroscopy, FTIR and RAMAN spectroscopy	Functional groups of GO: O-OH, C=O, C-OH and C-O.	Tewatia et al. (2020)
rGO	Improved Hummer's method and reduction by fresh ginger and garlic extracts.	Nanosheets	XRD, FTIR, TEM, RAMAN spectroscopy and UV–visible spectroscopy	Functional groups of GO: O-OH, C=O and C-O.	Rattan et al. (2020)
Ag NPs-F-rGO	Hummer's method and reduction by <i>Capparis spinosa</i> fruit extract.	Sheets morphology	FTIR, XRD, VSM, TEM and SEM	Functional groups of GO: O-OH, C=O, C-O, C=C and C-O-C.	Zarei et al. (2021)
L-rGO	Hummer's method and reduction by <i>Lycium barbarum</i> extract.	Nanosheets	XRD, TEM, SEM, FTIR, XPS, RAMAN spectroscopy and TGA	C/O ratio (GO): 1.35 C/O ratio (L-rGO): 6.5 C/O ratio (H-rGO): 6.6	Hou et al. (2017)
rGO	Hummer's method and reduction by green tea extract	Multi-layered sheets	SEM, FTIR, UV–visible spectroscopy and electrochemical sensing of SY	Functional groups of GO: O-OH, C=O and C-O.	Vatandost et al. (2020)
rGO	Modified Hummer's method and reduction by <i>Esfand</i> seed (ES) extract (ESE).	Nanosheets	XRD, FE-SEM, TGA, FTIR, RAMAN spectroscopy and EDS	C/O ratio (GO): 0.33 C/O ratio (rGO): 0.18	Ramezanzadeh et al. (2020)
rGO-Ag/ZnO	L-Methionine (L-Met) as green reductants and stabilizing agent.	Mixed morphologies of spherical, rose flower-petal, and hexagonal shape	SEM/EDS, TEM, XRD and UV - DRS	85% of degradation of MB after 210 min of irradiation.	Belachew et al. (2020)



Fig. 5. Schematic diagram of the main types of green reducing agents for the synthesis of rGO.

Lyceum barbarum extract as a green and natural reducing agent. GO was synthesized by the Hummer's method, followed by its reduction through the use of *Lyceum barbarum*, as a reducing agent. The material obtained was characterized by XRD, TEM, SEM, FTIR, XPS, RAMAN spectroscopy and TGA analyses. SEM analysis indicated a nanosheet-like morphology, which is characteristic of rGO. FTIR analysis indicated a decrease in peak intensity for functional groups containing oxygen, which confirmed the reduction of GO. The study pointed out that the mechanism of GO reduction was possible due to the active components present in *Lyceum barbarum* fruits, as they have a high affinity of binding to groups containing oxygen to form their corresponding oxides and other by-products. The rGO reduced by *Lyceum barbarum* had a C/O ratio of 6.5, while the rGO reduced by hydrazine hydrate had a C/O ratio of 6.6.

The C/O ratio obtained by Hou et al. (2017) for the rGO reduced by the natural agent *Lyceum barbarum* (6.5) is very close to the C/O ratio obtained by the use of hydrazine hydrate, which indicates that the natural agent has a reduction capacity comparable to the hydrazine hydrate. Through this study, it can be concluded that GO was effectively reduced by *Lyceum barbarum*.

Zarei et al. (2021) accomplished the synthesis of the green nanocomposite Ag NPs-F-rGO using the fruit extract of *Capparis spinosa* as a reducing agent. GO was synthesized by the Hummer's method. The Ag⁺ ions were coordinated with GO and then reduced by the fruit extract *Capparis spinosa* forming the AgNPs, which was converted to form rGO. The nanomaterial obtained was characterized by the analyzes of FTIR, TEM, SEM, and XRD. The FTIR analysis showed the existence of functional groups with oxygen, thus confirming the formation of the GO structure. The XRD analysis confirmed the presence of the characteristic peaks of rGO, and through SEM analysis sheets morphology was observed. The results indicated that *Capparis spinosa* is a promising reducing agent for the GO reduction.

Vatandost et al. (2020) performed the green synthesis of rGO by using green tea extract as a reducing and stabilizing agent. GO was synthesized by the Hummer's method, followed by its reduction using green tea extract. The nanomaterial obtained was characterized by SEM, FTIR, UV-visible spectroscopy and electrochemical sensing of SY

techniques. SEM analysis showed a morphology with multi-layered sheets on top of each other, rough surface and wavy structures, complying with the UV-visible spectroscopy analysis, which confirmed the formation of rGO. The FTIR analysis showed a decrease in the intensity of the peaks belonging to the hydroxyl groups of the GO, which indicates a successful reduction of the GO. The results revealed that the green tea extract acted not only as a reducing agent, but also as a functionalizing agent for the rGO structure.

Ramezanzadeh et al. (2020) obtained rGO by using *Esfand* seed extract (ESE) as green reducing agents. GO was synthesized by the modified Hummer's method, followed by its reduction using ESE. The rGO-ESE sheets were modified by metallic zinc ions, thus obtaining the rGO-ESE-Zn(II) sheets. The nanomaterial obtained was characterized by XRD, FE-SEM, TGA, FTIR, RAMAN spectroscopy and EDS analyses. The results of Raman, FE-SEM, EDS and FTIR analyzes indicated the disappearance of the carbonyl absorption peak, which confirmed the GO reduction. The XDR analysis revealed a significant increase in the D-spacing of the GO leaves after interaction with ESE-Zn(II). The calculated C/O ratio for GO was 0.33 and the C/O ratio for rGO was 0.18. This result indicates that the GO was reduced by the ESE molecules, in addition, the ESE was absorbed by the GO sheets, which resulted in an increase in the oxygen content.

The studies reported in this subsection pointed out that GO syntheses, as well as their reductions through the use of green reducing agents, were performed successfully. The results of the characterization analyzes indicated that reduced graphene oxide (rGO) was obtained, without any loss of its properties. The green reducing agents used in the studies present themselves as ecologically correct and low-cost methodologies for green GO reduction, thus replacing the use of traditional reducing agents, such as hydrazine and sodium borohydride, which are potentially toxic. Based on the results and discussions presented, it can be concluded that the use of natural reducers are a simple and economical method for the preparation of rGO, thus contributing to minimize the generation of toxic effluents during the synthesis processes.

5.3. Application of green synthesized nanomaterials for PAHs removal

Some green and low-cost methodologies have been developed over the years to remove petrogenic PAHs from wastewater. Crisafully et al. (2008) conducted a study to investigate the removal efficiency of PAHs using low-cost natural adsorbents, such as sugar cane bagasse, green coconut shells, chitin, and chitosan. The adsorptive process of PAHs (PRY, ANT, ACE, NAP) occurred under the following operational conditions: initial concentration of PAHs 5.0–15.0 mg L⁻¹, room temperature (28 ± 2 °C) and pH 7.5. The equilibrium experimental data had a better adjustment to Freundlich's model. Green coconut shells showed the best efficiency in removing PAHs from wastewater. A comparative performance analysis was also carried out with conventional adsorbents, such as activated carbon, cellulose, silica, and Amberlite T. The results indicated that green coconut shells and sugar cane bagasse were more efficient for the removal of PAHs from wastewater, than silica and Amberlite T.

Younis et al. (2014) accomplished the adsorption of PAHs from the oil industry wastewater using residual biomass from rice straw (RS) and sugar cane bagasse (SB), as low cost bioadsorbents. The bioadsorbents were applied to remove NAP, ANT and PYR, so that the adsorption experiments were conducted by batch adsorption, taking into account factors such as PAH concentration, temperature and contact time. The experimental kinetic data, for NAP, followed the PFO model, while for ANT and PYR, the kinetic data followed the PSO model, indicating that the physisorption and chemisorption were the determining mechanisms in the adsorptive process. The adsorption isotherms had a better fit and greater accuracy to the Langmuir's model, for all PAHs analyzed. By calculating the thermodynamic parameters, the nature of the adsorptive processes was determined. The results indicated that the bioadsorptive

process had a non-spontaneous nature ($\Delta G^\circ > 0$), good affinity for the adsorbate ($\Delta S^\circ > 0$) and endothermic nature ($\Delta H^\circ > 0$), indicating a strong interaction between bioadsorbents and PAHs. The adsorption results confirmed that the SB showed higher PAH adsorption efficiency than the RS.

The results obtained through the studies developed by Crisafully et al. (2008) and Younis et al. (2014) pointed out sugar cane bagasse as a simple and low-cost bioadsorbent for the remediation of PAHs from effluents from the petroleum industry.

The synthesis of green magnetic nanomaterials have been in the spotlight in the current context, due to their potential application in the removal of inorganic and organic compounds, such as PAHs, from domestic and industrial effluents (Nasrollahzadeh et al., 2020). Inbaraj et al. (2021) carried out the green synthesis of a magnetic activated carbon by using green tea leaves (MNPs-GTAC), aiming at its application for the remediation of BaA, BbF, CHR and BaP, from wastewater. The material obtained was characterized by the BET-N₂ method, XRD, FTIR, SEM/TEM, TGA and SQUID-VSM analyses. The kinetics experimental data was better adjusted to the PSO model, reaching 80% removal in 5 min. The equilibrium experimental data had a better adjustment to the Langmuir's model and had the following maximum adsorption capacities: 28.08 mg g⁻¹ for BbF, 22.75 mg g⁻¹ for CHR, 19.14 mg g⁻¹ for BaP and 15.86 mg g⁻¹ for BaA. Through the thermodynamic studies it was found that the nature of the adsorptive process was endothermic and spontaneous.

Shanker et al. (2017) presented in their studies a green synthesis method of an iron hexacyanoferrate nanostructure (FeHCF) using *Sapindus-mukorossi* as a natural surfactant. The TEM analysis showed that the nanoparticles have a hexagonal, rod and spherical shape. The XRD analysis showed a high crystallinity of the synthesized material. The nanomaterials were applied to the photocatalytic degradation and adsorption of PAHs from wastewater (ANT, PHEN, CHR, FLU and BaP), under the following operational conditions: 50 mg L⁻¹ of initial concentration of PAHs, dosage of adsorbent 25 mg, neutral pH and solar radiation. FeHCFs generated a significant reduction in PAHs (70–90% of reduction).

Hassan et al. (2018) effected the green synthesis of iron oxide nanoparticles (IONPs) by using extract from pomegranate peel. The nanomaterial obtained was applied in the adsorption of BaP and PYR from synthetic wastewater. Through the XRD analysis, the characteristic peaks of the iron oxide nanoparticles were observed, indicating that the amorphous structure of Fe₂O₃ was obtained. The factors that were evaluated in the adsorption of PAHs are: concentration of PAHs, dosage of adsorbent, pH and temperature. The maximum adsorption capacities of IONPs obtained was 0.029 and 2.8 mg g⁻¹ for BaP and PYR, respectively. Through the thermodynamic study, it was determined that the adsorptive process was spontaneous and exothermic, the kinetic data obtained had a better adjustment to the PSO model and the equilibrium data had a better adjustment to Langmuir's model. IONPs showed 98.5% of reduction for PRY and 99% for BaP.

The studies developed by Inbaraj et al. (2021), Shanker et al. (2017) and Hassan et al. (2018) successfully performed the green synthesis of magnetic nanoparticles using natural extracts. The green magnetic nanoparticles synthesized in the studies were applied in the adsorption of PAHs from wastewater and the results indicated high removal efficiency of PAHs in all studies. In the study developed by Li et al. (2017), the conventional synthesis of magnetic nanoparticles was carried out aiming its application in the adsorption of PAHs from wastewater. The results revealed an efficiency of removal of PAHs superior to 80%, for ANT and PHEN. Comparing the removal efficiencies of green magnetic nanoparticles with conventional ones, it can be concluded that the use of green nanomaterials presents itself as a simple, sustainable, promising and low-cost methodology for the adsorption of organic contaminants.

Due to the polluting and toxic effects of PAHs to the environment, some studies have been developed aiming at the application of green graphene-based nanomaterials for the remediation of these

contaminants from wastewater. Xiao et al. (2017) synthesized a graphene-like material through the carbonization and activation of sugar cane, which was applied for the removal of NAP, PHEN and 1-naphthol from wastewater. The morphological analysis indicated the obtaining of a turbostratic monolayer of graphene nanosheets and the results of FTIR and XPS showed the presence of the functional groups characteristic of GO. The adsorptive experiments were conducted in batch and the results showed an adsorption capacity of 615.8, 431.2 and 2040 mg g⁻¹ for NAP, PHEN and 1-naphthol, respectively. The equilibrium experimental data had a better adjustment to Freundlich's model.

Cheng et al. (2019) proposed an innovative and green route to synthesis of a material through hydrothermal treatment, followed by an activation by KHCO₃, to transform crop residues, rape straw and corn cob into an adsorbent called porous carbons (PCs). The material characterizations using SEM, XRD, RAMAN spectroscopy and FTIR techniques indicated the presence of graphene in its structure, through the abundant presence of C=C, in addition, the material presented the morphology of graphene sheets, which is characteristic of graphene. The XRD analysis showed the presence of the hexagonal structure characteristic of graphite, confirming its existence in the structure, which made it possible to increase the adsorption capacity through π - π interactions with PAHs. The materials obtained were applied to the adsorption of NAP, ACE and PHEN from wastewater. The adsorption experiments were performed in batch and the kinetic and equilibrium experimental data had a better fit to the PSO and Freundlich's models, respectively. The maximum adsorption capacities for PAHs were 592.97, 480.27, and 692.27 mg g⁻¹ for NAP, ACE and PHEN, respectively.

The experimental data of PAHs adsorption obtained in the study by Xiao et al. (2017) indicated that a graphene-like material, synthesized from sugar cane biomass, may have a high capacity for adsorption of PAHs from effluents. Comparing the adsorptive performance of the green GO, synthesized by Xiao et al. (2017), with the GO obtained in the study developed by Wang et al. (2014), using the conventional Hummer's method, in which an adsorption capacity of 68.66 and 69.86 mg g⁻¹ was obtained for NAP and PHEN, respectively, the superiority of the material obtained by the green route is evidenced. The results obtained by Cheng et al. (2019) also showed that GO synthesized by the green route is an ecological and promising adsorbent for the remediation of PAHs from wastewater.

5.4. Comparison with other PAHs removal technologies

Besides the adsorptive processes, many technologies, such as bioremediation, membrane separation, coagulation-flocculation and chemical oxidation processes (see Fig. S3), have been developed aiming at the remediation of petrogenic PAHs wastewater. Table 9 summarizes PAHs treatment technologies, as well the efficiency of removal.

The bioremediation processes consists of using microorganisms to remove pollutants, through its metabolic activity. Bioremediation has presented itself as a promising, sustainable, efficient and low-cost solution for the remediation of petrogenic PAHs from wastewater (Behera et al., 2018). Despite the advantages of bioremediation, the main limitations to be overcome are related to the low bioavailability of pollutants, low microbial adaptability, the need for a long residence time and large area (Shahsavari et al., 2019). Sun et al. (2019) reported, in their study, the PAHs removal from coke wastewater using the strain *Pseudomonas aeruginosa* S5 to produce the biosurfactant. The effect of the biosurfactant on the solubility of three HMW PAHs (PHEN, FLU, BaP) was evaluated. The results indicated that when the biosurfactant concentration exceeded the established critical micellar concentration (CMC), there was a linear increase in the solubility of the evaluated PAHs. The results also showed that the addition of *P. aeruginosa* S5 to the coke wastewater led to a 55% of reduction in the concentration of PAHs in 15 days, from 9141.02 to 5117.16 $\mu\text{g L}^{-1}$.

PAHs can also be removed from wastewater through the application

Table 9
Evaluation of the efficiency of different PAH removal techniques.

PAHs	Sources	Treatment techniques	PAHs Removal	References
PHEN, FLT and BAP	Coking Water	Bioremediation	Reduction from 9141.02 to 5117.16 $\mu\text{g L}^{-1}$ (55% of reduction)	Sun et al. (2019)
PHEN	Synthetic industrial wastewater	Microfiltration- H_2O_2 /UV-Catalytic wet peroxide oxidation	85% of reduction	Márquez et al. (2015)
ACE, PHEN, CHR and PYR	Municipal wastewater	Bioremediation- Microfiltration + UV disinfection	43 ± 14% of reduction	Qiao et al. (2019)
NAP, ACE, PHEN, FLT, ANT and PYR	Synthetic wastewater	Adsorption + Coagulation-flocculation	37.4–100% of reduction	Shabeer et al. (2014)
NAP and PYR	Synthetic wastewater	Chemical oxidation – Using Electrochemical oxidation and Fenton oxidation	Electrochemical oxidation: 80 – 81% of reduction; Fenton oxidation: 46% of reduction	Tran et al. (2010)
ANT and PYR	Synthetic wastewater	Activated carbon	Maximum removal of > 99% (after 4 h of contact)	Rasheed et al. (2015)
ANT	Synthetic wastewater	Adsorption by nitrogen-doped reduced graphene oxide (NRGO)	Adsorption capacities: 5.77 mg g^{-1} ; Adsorption efficiency: 58%	Song et al. (2021)
NAP, PHEN and PYR	Synthetic wastewater	Adsorption by graphene oxide/ Ag_3PO_4 (GO/ Ag_3PO_4)	82,1–100% of reduction (in 7.5 h)	Yang et al. (2018)

of different membrane separation technologies. The pressure-driven membrane processes are divided into three types: microfiltration (Goswami et al., 2019), ultrafiltration (Smol and Makula, 2012) and reverse osmosis (Smol et al., 2015). Membrane separation processes main advantages are lower energy consumption, less risk of pollution and low cost of reprocessing. However, the use of a single separation technique may not be a good efficient solution for removing contaminants, so they are usually used in combination with other methods. Some processes apply, for example, ultrafiltration in conjunction with reverse osmosis or even ultrafiltration combined with microfiltration, among other methods (Yu et al., 2017). Márquez et al. (2015) evaluated the viability of a multi-barrier treatment (MBT) for the remediation of PHEN, orange II, phenol and 4-chlorophenol from synthetic industrial wastewater. Following the MBT methodology, a pre-treatment of the effluent was carried out by microfiltration membrane (MF), and then, hydrogen peroxide (H_2O_2 /UVC) photolysis using a medium pressure Hg Lamp (MP) and granulated activated carbon (GAC). The results showed a degradation of 85% of the contaminants after the MBT treatment, thus generating a reduction in the toxicity of the effluents after the MF treatment.

Coagulation-flocculation is a physical-chemical process that can be used to remove colloidal suspensions and to eliminate organic compounds, such as PAHs, from water and wastewater (Smol and Makula, 2017). This technique has as main advantages: easy operation, low operating cost and simple equipment. The main limitations of these methods concern the treatment of oily wastewater due to the characteristics of the components dissolved in the oil mixture, which increases the complexity of the treatment, requiring the combination of this treatment with other methods. In addition, the treatment of oily wastewater can result in secondary pollution of water bodies, which can hinder treatment by the coagulation-flocculation technique (Zhao et al., 2021). Shabeer et al. (2014) conducted a study aimed at removing PAHs (NAP, ACE, PHEN, FLT, ANT and PYR) from wastewater. The effluent treatment process involved the PAHs adsorption by organo-modified nano-clays, then a coagulation-flocculation treatment was performed with alum and poly aluminum chloride (PAC). The application of the combined adsorption and coagulation-flocculation methods resulted in an effective and relatively simple methodology for the remediation of PAHs, obtaining a reduction between 37–100%.

PAHs concentration in wastewater can also be reduced through the application of advanced oxidation processes (AOPs). AOPs involve the application of different chemical reagents in order to increase the formation of radicals, generating the degradation of the compound of interest, allowing its remediation of the environment. These processes are presented as a viable technique for the removal of contaminants, as they enable high efficiency, relatively short remediation time and can be applied to different concentrations of pollutants. However, it is an expensive process, in addition, they can form intermediate compounds

resistant to their complete chemical degradation, which can prolong the treatment time (Ferrarese et al., 2008; Smol and Makula, 2017). Haneef et al. (2020), in their studies, evaluated the use of nanoscale zero valent iron (nZVI) and H_2O_2 to remove PAHs from produced water collected in an oil and gas exploration field in the South East Asian. The process was carried out in batch and the concentration of nZVI and H_2O_2 , pH and reaction time, had their effect evaluated. Central Composite Design (CCD) planning was applied through the response surface methodology (RSM), aiming at obtaining the optimum operating conditions of the remediation process. The experimental results showed a maximum removal of 89.5% for PAHs and 75.3% for chemical oxygen demand (COD). The ideal conditions obtained by the CCD were: 4.35 g L^{-1} and 1.60 g L^{-1} concentrations of nZVI and H_2O_2 respectively, 2.94 pH and 199.9 min reaction time.

Compared to other remediation technologies, adsorptive processes are presented as a simple, fast and efficient technology for the remediation of PAHs. Various types of adsorbents can be used for PAHs removal, such as activated carbon (Rasheed et al., 2015), organobentonite (Wu and Zhu, 2012), zeolites (Wolowicz et al., 2017), silica-based mesoporous materials (SBMM) (Yuan et al., 2018), graphene-based nanomaterials (Song et al., 2021). It is important to highlight that during the process of developing an adsorbent material it is necessary to study the kinetics, equilibrium and thermodynamics of adsorption.

The main challenges to be overcome by the adsorptive processes concern the development of ecologically correct and efficient methodologies for the synthesis of adsorbent materials, thus aiming to minimize the toxic effects caused by the excessive use of chemical reagents. The articles discussed in this review pointed out adsorption as an efficient and promising technique for PAH removal, when compared to other remediation technologies.

6. Challenges, future prospects and conclusions

This review addressed the main sources and harmful effects caused by the presence of PAHs in the environment, as well as the different technologies applied to remove them from wastewater in recent decades (2008–2021). Although they are generally found in lower concentrations, PAHs can cause irreversible damage to the environment and to humans, due to their high potential for genotoxicity, mutagenicity and carcinogenicity. This review covered the main studies on the adsorption of PAHs from wastewater by graphene-based nanomaterials, synthesized by conventional and green routes. Different methodologies for the synthesis of graphene-based adsorbents were discussed. The adsorptive processes were compared with other conventional remediation technologies, and presented themselves as more economical and efficient for the removal of petrogenic PAHs from wastewater.

The adsorption of different types of PAHs by different adsorbents was

discussed, considering the efficiency of kinetic, equilibrium, thermodynamic and breakthrough curve parameters. The studies approached indicated, by means of the maximum adsorption capacities, that the removal efficiency for each type of PAHs depends on the effect of pH, contact time, temperature, concentration and affinity for adsorbate. Most of the adsorptive processes evaluated were spontaneous in nature and chemisorption was the main mechanism associated with the processes, since most kinetic data had a better adjustment to the PSO's model. Batch and fixed-bed adsorptive processes were also evaluated.

Different methodologies for the green synthesis of nanomaterials were addressed, due to the great relevance of this topic for the present time. The studies discussed showed the reduction of GO through the use of green reducing agents, such as plant extracts, microorganisms and biomass residues, as a sustainable, simple and low-cost method for the synthesis of rGO. The adsorption of PAHs through the use of green nanomaterials had an adsorption capacity comparable to the conventional nanomaterials. However, it is also important to highlight that there are still many challenges to be overcome by green synthesis processes, especially with regard to the process efficiency and the structural and thermal properties of green materials. Despite the growing number of studies that address the application of green nanomaterials to remove PAHs, there are still gaps in the literature about the application of green reduced GO for the removal of petrogenic PAHs from wastewater. In this context, some perspectives for future studies can be addressed, such as: (i) Study of the adsorptive properties of green rGO for the remediation of wastewater PAHs; (ii) Studies on the reuse/regeneration of green nano-adsorbents; (iii) Application of green adsorbents in dynamic fixed-bed systems; (iv) Economic analysis of costs for application in large-scale adsorptive systems aiming industrial use; (v) Life cycle analysis for the synthesis of the adsorbent and the adsorptive process in order to assess the environmental impact.

Declaration of Competing Interest

The authors declare that they have no known competing financial interests or personal relationships that could have appeared to influence the work reported in this paper.

Acknowledgements

The authors of this paper are grateful for the financial support of the Human Resources Training Program for the Oil, Natural Gas and Bio-fuels Sector (PRH-ANP) (Number 29), Brazilian National Research Council (CNPq) (Grant #308046/2019-6 and Grant #141469/2018-8), São Paulo Research Foundation (FAPESP) (Grant #2019/11353-8; #2019/07822-2) and Coordination for the Improvement of Higher Education Personnel (CAPES) (Finance Code 001).

Appendix A. Supporting information

Supplementary data associated with this article can be found in the online version at [doi:10.1016/j.jhazmat.2021.126904](https://doi.org/10.1016/j.jhazmat.2021.126904).

References

- Abdel-Shafy, H.I., Mansour, M.S.M., 2016. A review on polycyclic aromatic hydrocarbons: source, environmental impact, effect on human health and remediation. *Egypt. J. Pet.* 25, 107–123. <https://doi.org/10.1016/j.ejpe.2015.03.011>.
- Abdullahi, B.O., Ahmed, E., Abdulgader, H.A., Alghunaimi, F., Saleh, T.A., 2021. Facile fabrication of hydrophobic alkylamine intercalated graphene oxide as adsorbent for highly effective oil-water separation. *J. Mol. Liq.* 325, 115057 <https://doi.org/10.1016/j.molliq.2020.115057>.
- Adeniji, A.O., Okoh, O.O., Okoh, A.I., 2018. Analytical Methods for Polycyclic Aromatic Hydrocarbons and their Global Trend of Distribution in Water and Sediment: A Review. In: Zoveidavianpoor, M. (Ed.), *Recent Insights in Petroleum Science and Engineering*. IntechOpen, pp. 393–428.
- Adeola, A.O., Forbes, P.B.C., 2019. Optimization of the sorption of selected polycyclic aromatic hydrocarbons by regenerable graphene wool. *Water Sci. Technol.* 80, 1931–1943. <https://doi.org/10.2166/wst.2020.011>.
- Albayati, T.M., Kalash, K.R., 2020. Polycyclic aromatic hydrocarbons adsorption from wastewater using different types of prepared mesoporous materials MCM-41 in batch and fixed bed column. *Process Saf. Environ. Prot.* 133, 124–136. <https://doi.org/10.1016/j.psep.2019.11.007>.
- Alghunaimi, F.I., Alsaeed, D.J., Harith, A.M., Saleh, T.A., 2019. Synthesis of 9-octadecenoic acid grafted graphene modified with polystyrene for efficient light oil removal from water. *J. Clean. Prod.* 233, 946–953. <https://doi.org/10.1016/j.jclepro.2019.05.239>.
- Alkhouzaam, A., Qiblaweya, H., Khraisheha, M., Atieh, M., Al-Ghouti, M., 2020. Synthesis of graphene oxides particle of high oxidation degree using a modified Hummers method. *Ceram. Int.* 46, 23997–24007. <https://doi.org/10.1016/j.ceramint.2020.06.177>.
- Álvarez, I.M., Menach, K.L., Devier, M.H., Barbarin, I., Tomovska, R., Cajaraville, M.P., Budzinski, H., Orbea, A., 2021. Uptake and effects of graphene oxide nanomaterials alone and in combination with polycyclic aromatic hydrocarbons in zebrafish. *Sci. Total Environ.* 775, 145669 <https://doi.org/10.1016/j.scitotenv.2021.145669>.
- Akinpelu, A.A., Ali, M.E., Johan, M.R., Saidur, R., Chowdhury, Z.Z., Shamsi, A.M., Saleh, T.A., 2019. Effect of the oxidation process on the molecular interaction of polyaromatic hydrocarbons (PAH) with carbon nanotubes: adsorption kinetic and isotherm study. *J. Mol. Liq.* 289, 111107 <https://doi.org/10.1016/j.molliq.2019.111107>.
- Andrade, J.R., Oliveira, M.F., Canevesi, R.L.S., Landers, R., Silva, M.G.C., Vieira, M.G.A., 2020. Comparative adsorption of diclofenac sodium and losartan potassium in organophilic clay-packed fixed-bed: X-ray photoelectron spectroscopy characterization, experimental tests and theoretical study on DFT-based chemical descriptors. *J. Mol. Liq.* 312, 113427 <https://doi.org/10.1016/j.molliq.2020.113427>.
- Asha, A.B., Narain, R., 2020. Nanomaterials properties. In: Narain, R. (Ed.), *Polymer Science and Nanotechnology*. Elsevier Inc, Canada, pp. 343–359.
- Bagri, A., Mattevi, C., Acik, M., Chabal, Y.J., Chhowalla, M., Shenoy, V.B., 2010. Structural evolution during the reduction of chemically derived graphene oxide. *Nat. Chem.* 2, 581–587. <https://doi.org/10.1038/nchem.686>.
- Balati, A., Shahbazi, A., Amini, M.M., Hashemi, S.H., 2015. Adsorption of polycyclic aromatic hydrocarbons from wastewater by using silica-based organic-inorganic nanohybrid material. *J. Water Reuse Desalin.* 5 (1), 50–63. <https://doi.org/10.2166/wrd.2014.013>.
- Behara, B.K., Das, A., Sarkar, D.J., Weerathunge, P., Parida, P.K., Das, B.K., Thavamani, P., Ramanathan, R., Bansal, V., 2018. Polycyclic Aromatic Hydrocarbons (PAHs) in inland aquatic ecosystems: perils and remedies through biosensors and bioremediation. *Environ. Pollut.* 241, 212–233. <https://doi.org/10.1016/j.envpol.2018.05.016>.
- Belachew, N., Kabsay, M.H.K., Tadesse, A., Basavaiah, K., 2020. Green synthesis of reduced graphene oxide grafted Ag/ZnO for photocatalytic abatement of methylene blue and antibacterial activities. *J. Environ. Chem. Eng.* 8, 104106 <https://doi.org/10.1016/j.jece.2020.104106>.
- Beyer, J., Goksoyr, A., Hjermmann, D.O., Klungsoyr, J., 2020. Environmental effects of offshore produced water discharges: a review focused on the Norwegian continental shelf. *Mar. Environ. Res.* 162, 105–155. <https://doi.org/10.1016/j.marenvres.2020.105155>.
- Bolade, O.P., Williams, A.B., Benson, N.U., 2020. Green synthesis of iron-based nanomaterials for environmental remediation: a review. *Environ. Nanotechnol. Monit. Manag.* 13, 100279 <https://doi.org/10.1016/j.enmm.2019.100279>.
- Bohart, G.S., Adams, E.Q., 1920. Some aspects of the behavior of charcoal with respect to chlorine. *J. Am. Chem. Soc.* 42, 523–544. <https://doi.org/10.1021/ja01448a018>.
- Brodie, B.C., 1859. On the atomic weight of graphite. *Philos. Trans. R. Soc. Lond.* 149, 249–259. <https://doi.org/10.1098/rstl.1859.0013>.
- Chakravarty, R., Dash, A., 2013. Role of nanoporous materials in radiochemical separations for biomedical applications. *J. Nanosci. Nanotechnol.* 13, 2431–2450. <https://doi.org/10.1166/jnn.2013.7349>.
- Chen, J., Yao, B., Li, C., Shi, G., 2013. An improved Hummers method for eco-friendly synthesis of graphene oxide. *Carbon* 64, 225–229. <https://doi.org/10.1016/j.carbon.2013.07.055>.
- Chen, W.H., Huang, J.R., 2020. Adsorption of organic including pharmaceutical and inorganic contaminants in water toward graphene-based materials. In: Maldonado, A.J.H., Blaney, L. (Eds.), *Contaminants of Emerging Concern in Water and Wastewater*. Elsevier Inc, pp. 93–113.
- Cheng, H., Bian, Y., Wang, F., Jiang, X., Ji, R., Gu, C., Yang, X., Song, Y., 2019. Green conversion of crop residues into porous carbons and their application to efficiently remove polycyclic aromatic hydrocarbons from water: sorption kinetics, isotherms and mechanism. *Bioresour. Technol.* 284, 1–8. <https://doi.org/10.1016/j.biortech.2019.03.104>.
- Chua, C.K., Pumeria, M., 2014. Chemical reduction of graphene oxide: a synthetic chemistry viewpoint. *Chem. Soc. Rev.* 43, 291–312. <https://doi.org/10.1039/c3cs60303b>.
- Crisafulli, R., Milhome, M.A.L., Cavalcante, R.M., Silveira, E.R., Keukeleire, D.D., Nascimento, R.F., 2008. Removal of some polycyclic aromatic hydrocarbons from petrochemical wastewater using low-cost adsorbents of natural origin. *Bioresour. Technol.* 99, 4515–4519. <https://doi.org/10.1016/j.biortech.2007.08.041>.
- Duan, H., Wang, D., Li, Y., 2015. Green chemistry for nanoparticle synthesis. *Chem. Soc. Rev.* 44, 5778–5792. <https://doi.org/10.1039/c4cs00363b>.
- Eshwarasinghe, D., Loganathan, P., Kalaruban, M., Sountharajah, D.P., Kandasamy, J., Vigneswaran, S., 2018. Removing polycyclic aromatic hydrocarbons from water using granular activated carbon: kinetic and equilibrium adsorption

- studies. *Environ. Sci. and Pollut. Res.* 25, 13511–13524. <https://doi.org/10.1007/s11356-018-1518-0>.
- Fadillah, G., Saleh, T.A., Wahyuningsih, S., Putri, E.N.K., Febrianastuti, S., 2019. Electrochemical removal of methylene blue using alginate-modified graphene adsorbents. *Chem. Eng. J.* 378, 122140 <https://doi.org/10.1016/j.cej.2019.122140>.
- Ferrarese, E., Andreottola, G., Oprea, I.A., 2008. Remediation of PAH-contaminated sediments by chemical oxidation. *J. Hazard. Mater.* 152, 128–139. <https://doi.org/10.1016/j.jhazmat.2007.06.080>.
- Freundlich, H.M.F., 1906. Over the adsorption in solution. *Urnal Phys. Chem.* 57, 385–471.
- Ghosal, D., Ghosh, S., Dutta, T.K., Ahn, Y., 2016. Current state of knowledge in microbial degradation of polycyclic aromatic hydrocarbons (PAHs): a review. *Front. Microbiol.* 7, 1369. <https://doi.org/10.3389/fmicb.2016.01369>.
- Gomis, V.V., Grau, J., Benedé, J.L., Chisvert, A., Salvador, A., 2020. Reduced graphene oxide-based magnetic composite for trace determination of polycyclic aromatic hydrocarbons in cosmetics by stir bar sorptive dispersive microextraction. *J. Chromatogr. A* 1624, 461229. <https://doi.org/10.1016/j.chroma.2020.461229>.
- Goswami, L., Kumar, R.V., Pakshirajan, K., Pugazhenth, G., 2019. A novel integrated biodegradation—Microfiltration system for sustainable wastewater treatment and energy recovery. *J. Hazard. Mater.* 365, 707–715. <https://doi.org/10.1016/j.jhazmat.2018.11.029>.
- Gupta, H., Singh, S., 2018. Kinetics and thermodynamics of phenanthrene adsorption from water on orange rind activated carbon. *Environ. Technol. Innov.* 10, 208–214. <https://doi.org/10.1016/j.eti.2018.03.001>.
- Gupta, V.K., Srivastava, S.K., Mohan, D., Sharma, S., 1998. Design parameters for fixed bed reactors of activated carbon developed from fertilizer waste for the removal of some heavy metal ions. *Waste Manag.* 17, 517–522. [https://doi.org/10.1016/S0956-053X\(97\)10062-9](https://doi.org/10.1016/S0956-053X(97)10062-9).
- Hall, S., Tang, R., Baeyens, J., Dewil, R., 2009. Removing polycyclic aromatic hydrocarbons from water by adsorption on silicagel. *Polycycl. Aromat. Compd.* 29, 160–183. <https://doi.org/10.1080/10406630903017534>.
- Haneef, T., Mustafa, M.R.U., Rasool, K., Ho, Y.C., Kutty, S.R.M., 2020. Removal of polycyclic aromatic hydrocarbons in a heterogeneous fenton like oxidation system using nanoscale zero-valent iron as a catalyst. *Water* 12, 2430. <https://doi.org/10.3390/w12092430>.
- Hassan, S.S.M., Shafy, H.I.A., Mansour, M.S.M., 2018. Removal of pyrene and benzo(a) pyrene micropollutant from water via adsorption by green synthesized iron oxide nanoparticles. *Adv. Nat. Sci. Nanosci. Nanotechnol.* 9, 015006 <https://doi.org/10.1088/2043-6254/aaa6f0>.
- Hou, D., Liu, Q., Cheng, H., Zhang, H., Wang, S., 2017. Green reduction of graphene oxide via Lycium barbarum extract. *J. Solid State Chem.* 246, 351–356. <https://doi.org/10.1016/j.jssc.2016.12.008>.
- Huang, D., Xu, B., Wu, J., Brookes, P.C., Xu, J., 2019. Adsorption and desorption of phenanthrene by magnetic graphene nanomaterials from water: roles of pH, heavy metal ions and natural organic matter. *Chem. Eng. J.* 368, 390–399. <https://doi.org/10.1016/j.cej.2019.02.152>.
- Huang, Y., Zhang, W., Ruan, G., Li, X., Cong, Y., Du, F., Li, J., 2018. Reduced graphene oxide-hybridized polymeric high-internal phase emulsions for highly efficient removal of polycyclic aromatic hydrocarbons from water matrix. *Langmuir* 34, 3661–3668. <https://doi.org/10.1021/acs.langmuir.8b00005>.
- Hummers, W.S., Offeman, R.E., 1958. Preparation of graphitic oxide. *J. Am. Chem. Soc.* 80, 1339.
- Ho, Y.S., McKay, G., 1999. Pseudo-second order model for sorption processes. *Process Biochem.* 34, 451–465. [https://doi.org/10.1016/S0032-9592\(98\)00112-5](https://doi.org/10.1016/S0032-9592(98)00112-5).
- Inbaraj, B.S., Sridhar, K., Chen, B.H., 2021. Removal of polycyclic aromatic hydrocarbons from water by magnetic activated carbon nanocomposite from green tea waste. *J. Hazard. Mater.* 415, 125701 <https://doi.org/10.1016/j.jhazmat.2021.125701>.
- Kinniburgh, D.G., 1986. General purpose adsorption isotherms. *Environ. Sci. Technol.* 20, 895–904. <https://doi.org/10.1021/es00151a008>.
- Lagergren, S., 1898. About the theory of so-called adsorption of soluble substances. *K. Sven. Vetensk. Handl.* 24, 1–39.
- Lander, J.J., 1964. Chemisorption and ordered surface structure. *Surf. Sci.* 1, 125–164. [https://doi.org/10.1016/0039-6028\(64\)90024-X](https://doi.org/10.1016/0039-6028(64)90024-X).
- Langmuir, I., 1918. The adsorption of gases on plane surfaces of glass, mica and platinum. *J. Am. Chem. Soc.* 40, 1361–1403.
- Li, J., Zhou, Q., Liu, Y., Lei, M., 2017. Recyclable nanoscale zero-valent iron-based magnetic polydopamine coated nanomaterials for the adsorption and removal of phenanthrene and anthracene. *Sci. Technol. Adv. Mater.* 18, 3–16. <https://doi.org/10.1080/14686996.2016.1246941>.
- Mahmoud, A.E.D., 2020. Nanomaterials: green synthesis for water applications. In: Kharisova, O.V., Martínez, L.M.T., Kharisov, B.I. (Eds.), *Handbook of Nanomaterials and Nanocomposites for Energy and Environmental Applications*. Springer Nature, Switzerland, pp. 1–21. https://doi.org/10.1007/978-3-030-11155-7_67-1.
- Márquez, J.J.R., Herrera, M.G.P., Díaz, M.L.M., Merino, A.A., Manzano, M.A., 2015. Combined AOPs for potential wastewater reuse or safe discharge based on multi-barrier treatment (microfiltration-H₂O₂/UV-catalytic wet peroxide oxidation). *Chem. Eng. J.* 270, 80–90. <https://doi.org/10.1016/j.cej.2015.02.011>.
- Marczewska, A.D., Marczewski, A.W., 2002. Effect of adsorbate structure on adsorption from solutions. *Appl. Surf. Sci.* 196, 264–272. [https://doi.org/10.1016/S0169-4332\(02\)00064-8](https://doi.org/10.1016/S0169-4332(02)00064-8).
- Masood, N., Zakaria, M.P., Halimoon, N., Aris, A.Z., Magam, S.M., Kannan, N., Mustafa, S., Ali, M.M., Keshavarzifard, M., Vaezzadeh, V., Alkhadher, S.A.A., Al-Ordaini, N.A., 2016. Anthropogenic waste indicators (AWIs), particularly PAHs and LABs, in Malaysian sediments: application of aquatic environment for identifying anthropogenic pollution. *Mar. Pollut. Bull.* 102, 160–175. <https://doi.org/10.1016/j.marpolbul.2015.11.032>.
- Mercier, J.P., Zambelli, G., Kurz, W., 2002. Nanomaterials and nanostructured materials. In: Mercier, J.P., Zambelli, G., Kurz, W. (Eds.), *Introduction to Materials Science*. Elsevier Ltd, pp. 421–438. <https://doi.org/10.1016/B978-2-84299-286-6.50023-8>.
- Mortazavi, M., Baghdadi, M., Javadi, N.H.S., Torabian, A., 2019. The black beads produced by simultaneous thermal reducing and chemical bonding of graphene oxide on the surface of amino-functionalized sand particles: application for PAHs removal from contaminated waters. *J. Water Process Eng.* 31, 100798 <https://doi.org/10.1016/j.jwpe.2019.100798>.
- Mukhopadhyay, S., Dutta, R., Das, P., 2020. A critical review on plant biomaterials for determination of polycyclic aromatic hydrocarbons (PAHs) in air through solvent extraction techniques. *Chemosphere* 251, 126441. <https://doi.org/10.1016/j.chemosphere.2020.126441>.
- Mukweho, N., Gusain, R., Kankeu, E.F., Kumar, N., Waanders, F., Ray, S.S., 2020. Removal of naphthalene from simulated wastewater through adsorption-photodegradation by ZnO/Ag/GO nanocomposite. *J. Ind. Eng. Chem.* 81, 393–404. <https://doi.org/10.1016/j.jiec.2019.09.030>.
- Muscat, J.P., News, D.M., 1978. Chemisorption on metals. *Prog. Surf. Sci.* 9, 1–43. [https://doi.org/10.1016/0079-6816\(78\)90005-9](https://doi.org/10.1016/0079-6816(78)90005-9).
- Nasuhoglu, D., Rodayan, A., Berk, D., Yargeau, V., 2012. Removal of the antibiotic levofloxacin (LEVO) in water by ozonation and TiO₂ photocatalysis. *Chem. Eng. J.* 189–190, 41–48. <https://doi.org/10.1016/j.cej.2012.02.016>.
- Nasrollahzadeh, M., Sajjadi, M., Irvani, S., Varma, R.S., 2021. Green-synthesized nanocatalysts and nanomaterials for water treatment: current challenges and future perspectives. *J. Hazard. Mater.* 401, 123401 <https://doi.org/10.1016/j.jhazmat.2020.123401>.
- Nikitha, T., Satyaprakash, M., Vani, S., Sadhana, B., Padal, S.B., 2017. A review on polycyclic aromatic hydrocarbons: their transport, fate and biodegradation in the environment. *Int. J. Curr. Microbiol. Appl. Sci.* 6, 1627–1639. <https://doi.org/10.20546/ijcmas.2017.604.199>.
- Novoselov, K.S., Geim, A.K., Morozov, S.V., Jiang, D., Zhang, Y., Dubonos, S.V., Grigorieva, I.V., Firsov, A.A., 2004. Electric field effect in atomically thin carbon films. *Science* 306, 666–669. <https://doi.org/10.1126/science.1102896>.
- Pei, S., Cheng, H.M., 2012. The reduction of graphene oxide. *Carbon* 50, 3210–3228. <https://doi.org/10.1016/j.carbon.2011.11.010>.
- Pei, Z., Li, L., Sun, L., Zhang, S., Shan, X., Yang, S., Wen, B., 2013. Adsorption characteristics of 1,2,4-trichlorobenzene, 2,4,6-trichlorophenol, 2-naphthol and naphthalene on graphene and graphene oxide. *Carbon* 51, 156–163. <https://doi.org/10.1016/j.carbon.2012.08.024>.
- Perreault, F., Faria, A.F., Elimelech, M., 2015. Environmental applications of graphene-based nanomaterials. *Chem. Soc. Rev.* 44, 5861–5896. <https://doi.org/10.1039/c5cs00021a>.
- Plazinski, W., Rudzinski, W., Plazinska, A., 2009. Theoretical models of sorption kinetics including a surface reaction mechanism: a review. *Adv. Colloid Interface Sci.* 152, 2–13. <https://doi.org/10.1016/j.cis.2009.07.009>.
- Pokropivny, V.V., Skorokhod, V.V., 2007. Classification of nanostructures by dimensionality and concept of surface forms engineering in nanomaterial science. *Mater. Sci. Eng.* 27, 990–993. <https://doi.org/10.1016/j.msec.2006.09.023>.
- Qi, Y., Wang, C., Lv, C., Lun, Z., Zheng, C., 2017. Removal Capacities of Polycyclic Aromatic Hydrocarbons (PAHs) by a Newly Isolated Strain from Oilfield Produced Water. *Int. J. Environ. Res. Public Health* 14, 215. <https://doi.org/10.3390/ijerph14020215>.
- Qiao, M., Fu, L., Cao, W., Bai, Y., Huang, Q., Zhao, X., 2019. Occurrence and removal of polycyclic aromatic hydrocarbons and their derivatives in an ecological wastewater treatment plant in South China and effluent impact to the receiving river. *Environ. Sci. Pollut. Res.* 26, 5638–5644. <https://doi.org/10.1007/s11356-018-3839-4>.
- Ramezanzadeh, M., Bahlakeh, G., Ramezanzadeh, B., 2020. Green synthesis of reduced graphene oxide nanosheets decorated with zinc-centered metal-organic film for epoxy-ester composite coating reinforcement: DFT-D modeling and experimental explorations. *J. Taiwan Inst. Chem. Eng.* 114, 311–330. <https://doi.org/10.1016/j.jtice.2020.09.003>.
- Rasheed, A., Farooq, F., Rafique, U., Nasreen, S., Ashraf, M.A., 2015. Analysis of sorption efficiency of activated carbon for removal of anthracene and pyrene for wastewater treatment. *Desalin. Water Treat.* 57, 145–150. <https://doi.org/10.1080/19443994.2015.1015304>.
- Rani, M., Shanker, U., 2018. Remediation of Polycyclic Aromatic Hydrocarbons Using Nanomaterials. In: Crini, G., Lichtfouse, E. (Eds.), *Green Adsorbents for Pollutant Removal*. Springer, Cham, pp. 343–387.
- Rattan, S., Kumar, S., Goswami, J.K., 2020. Graphene oxide reduction using green chemistry. *Mater. Today Proc.* 26, 3327–3331. <https://doi.org/10.1016/j.matpr.2019.09.168>.
- Reghunadhan, A., Kalarikkal, N., Thomas, S., 2018. Mechanical Property Analysis of Nanomaterials. In: Bhagyaraj, S.M., Oluwafemi, O.S., Kalarikkal, N., Thomas, S. (Eds.), *Characterization of Nanomaterials*. Elsevier Ltd, pp. 191–212.
- Ruiz, D.A.P., Ávila, G.D., Suesca, C.A., Delgado, A.D.G., Herrera, A., 2020. Ionic cross-linking fabrication of chitosan-based beads modified with FeO and TiO₂ nanoparticles: adsorption mechanism toward naphthalene removal in seawater from cartagena bay area. *ACS Omega* 5, 26463–26475. <https://doi.org/10.1021/acsomega.0c02984>.
- Ruthven, D.M., 1984. Principles of Adsorption and Adsorption Processes. John Wiley & Sons, New York, NY.
- Saleh, T.A., Parthasarathy, P., Irfan, M., 2019. Advanced functional polymer nanocomposites and their use in water ultra-purification. *Trends Environ. Anal. Chem.* 24, e00067 <https://doi.org/10.1016/j.teac.2019.e00067>.

- Schweich, D., Sardin, M., 1981. Adsorption, partition, ion exchange and chemical reaction in batch reactors or in columns - a review. *J. Hydrol.* 50, 1–33. [https://doi.org/10.1016/0022-1694\(81\)90059-7](https://doi.org/10.1016/0022-1694(81)90059-7).
- Scurtu, C.T., 2009. Treatment of produced water: targeting dissolved compounds to meet a zero harmful discharge in oil and gas production. Thesis (Degree of Philosophiae Doctor) - Norwegian University of Science and Technology.
- Shabeer, T.P.A., Saha, A., Gajbhiye, V.T., Gupta, S., Manjajiah, K.M., Varghese, E., 2014. Removal of poly aromatic hydrocarbons (PAHs) from water: effect of nano and modified nano-clays as a flocculation aid and adsorbent in coagulation/flocculation process. *Polycycl. Aromat. Compd.* 34, 452–467. <https://doi.org/10.1080/10406638.2014.895949>.
- Shahsavari, E., Schwarz, A., Medina, A.A., Ball, A.S., 2019. Biological degradation of polycyclic aromatic compounds (PAHs) in soil: a current perspective. *Curr. Pollut. Rep.* 5, 84–92. <https://doi.org/10.1007/s40726-019-00113-8>.
- Shanker, U., Jassal, V., Rani, M., 2017. Green synthesis of iron hexacyanoferrate nanoparticles: potential candidate for the degradation of toxic PAHs. *J. Environ. Chem. Eng.* 5, 4108–4120. <https://doi.org/10.1016/j.jece.2017.07.042>.
- Sharma, A., Siddiqi, Z.M., Pathania, D., 2017. Adsorption of polyaromatic pollutants from water system using carbon/ZnFe₂O₄ nanocomposite: equilibrium, kinetic and thermodynamic mechanism. *J. Mol. Liq.* 240, 361–371. <https://doi.org/10.1016/j.molliq.2017.05.083>.
- Smol, M., Makula, M.W., 2012. Effectiveness in the removal of polycyclic aromatic hydrocarbons from industrial wastewater by ultrafiltration technique. *Arch. Environ. Prot.* 38, 49–58. <https://doi.org/10.2478/v10265-012-0040-6>.
- Smol, M., Makula, M.W., Mielczarek, K., Bohdziewicz, J., Wlók, D., 2015. The use of reverse osmosis in the removal of PAHs from municipal landfill leachate. *Polycycl. Aromat. Compd.* 36, 20–39. <https://doi.org/10.1080/10406638.2014.957403>.
- Smol, M., Makula, M.W., 2017. The effectiveness in the removal of PAHs from aqueous solutions in physical and chemical processes: a review. *Polycycl. Aromat. Compd.* 37, 292–313. <https://doi.org/10.1080/10406638.2015.1105828>.
- Song, T., Tian, W., Qiao, K., Zhao, J., Chu, M., Du, Z., Wang, L., Xie, W., 2021. Adsorption behaviors of polycyclic aromatic hydrocarbons and oxygen derivatives in wastewater on N-doped reduced graphene oxide. *Sep. Purif. Technol.* 254, 117565. <https://doi.org/10.1016/j.seppur.2020.117565>.
- Stankovich, S., Dikin, D.A., Dommett, G.H.B., Kohlhaas, K.M., Zimney, E.J., Stach, E.A., Piner, R.D., Nguyen, S.T., Ruoff, R.S., 2006. Graphene-based composite materials. *Nature* 442, 282–286. <https://doi.org/10.1038/nature04969>.
- Sun, S., Wanga, Y., Zang, T., Weib, J., Wua, H., Weib, C., Qiu, G., Lib, F., 2019. A biosurfactant-producing *Pseudomonas aeruginosa* S5 isolated from coking wastewater and its application for bioremediation of polycyclic aromatic hydrocarbons. *Bioresour. Technol.* 281, 421–428. <https://doi.org/10.1016/j.biortech.2019.02.087>.
- Sun, Y., Yang, S., Zhao, G., Wang, Q., Wang, X., 2013. Adsorption of polycyclic aromatic hydrocarbons on graphene oxides and reduced graphene oxides. *Chem. Asian J.* 8, 2755–2761. <https://doi.org/10.1002/asia.201300496>.
- Tewatia, K., Sharma, A., Sharma, M., Kumar, A., 2020. Synthesis of graphene oxide and its reduction by green reducing agent. *Mater. Today Proc.* 44, 3933–3938. <https://doi.org/10.1016/j.matpr.2020.09.294>.
- Thomas, H.C., 1944. Heterogeneous ion exchange in a flowing system. *J. Am. Chem. Soc.* 66, 1664–1666. <https://doi.org/10.1021/ja01238a017>.
- Tran, L.H., Drogui, P., Mercier, G., Blais, J.F., 2010. Comparison between Fenton oxidation process and electrochemical oxidation for PAH removal from an amphoteric surfactant solution. *J. Appl. Electrochem.* 40, 1493–1510. <https://doi.org/10.1007/s10800-010-0128-4>.
- Valderrama, C., Gamisans, X., Heras, X., Farran, A., Cortina, J.L., 2008. Sorption kinetics of polycyclic aromatic hydrocarbons removal using granular activated carbon: intraparticle diffusion coefficients. *J. Hazard. Mater.* 157, 386–396. <https://doi.org/10.1016/j.jhazmat.2007.12.119>.
- Vatandost, E., Saraei, A.G.H., Chekin, F., Raiesi, S.N., SHAHIDI, S.A., 2020. Green tea extract assisted green synthesis of reduced graphene oxide: application for highly sensitive electrochemical detection of sunset yellow in food products. *Food Chem. X* 6, 100085. <https://doi.org/10.1016/j.fochx.2020.100085>.
- Vert, M., Doi, Y., Hellwich, K.H., Hess, M., Hodge, P., Kubisa, P., Rinaudo, M., Schué, F., 2012. Terminology for biorelated polymers and applications (IUPAC Recommendations 2012). *Pure Appl. Chem.* 84, 377–410. <https://doi.org/10.1351/PAC-REC-10-12-04>.
- Wolowicz, M., Muir, B., Zięba, K., Bajda, T., Kowalik, M., Franus, W., 2017. Experimental study on the removal of VOCs and PAHs by zeolites and surfactant-modified zeolites. *Energy Fuels* 31, 8803–8812. <https://doi.org/10.1021/acs.energyfuels.7b01124>.
- Wang, J., Chen, Z., Chen, B., 2014. Adsorption of polycyclic aromatic hydrocarbons by graphene and graphene oxide nanosheets. *Environ. Sci. Technol.* 48, 4817–4825. <https://doi.org/10.1021/es405227u>.
- Wu, Z., Zhu, L., 2012. Removal of polycyclic aromatic hydrocarbons and phenols from coking wastewater by simultaneously synthesized organobentonite in a one-step process. *J. Environ. Sci.* 24, 248–253. [https://doi.org/10.1016/S1001-0742\(11\)60780-8](https://doi.org/10.1016/S1001-0742(11)60780-8).
- Xiao, X., Chen, B., Zhu, L., Schnoor, J.L., 2017. Sugar cane-converted graphene-like material for the superhigh adsorption of organic pollutants from water via coassembly mechanisms. *Environ. Sci. Technol.* 51, 12644–12652. <https://doi.org/10.1021/acs.est.7b03639>.
- Yang, X., Li, J., Wen, T., Ren, X., Huang, Y., Wang, X., 2013. Adsorption of naphthalene and its derivatives on magnetic graphene composites and the mechanism investigation. *Colloids Surf. A Physicochem. Eng. Asp.* 422, 118–125. <https://doi.org/10.1016/j.colsurfa.2012.11.063>.
- Yang, X., Cai, H., Bao, M., Yu, J., Lu, J., Li, Y., 2018. Insight into the highly efficient degradation of PAHs in water over graphene oxide/Ag₃PO₄ composites under visible light irradiation. *Chem. Eng. J.* 334, 355–376. <https://doi.org/10.1016/j.cej.2017.09.104>.
- Yoon, Y.H., Nelson, J.H., 1984. Application of gas adsorption kinetics I. A theoretical model for respirator cartridge service life. *Am. Ind. Hyg. Assoc. J.* 45, 509–516. <https://doi.org/10.1080/15298668491400197>.
- Younis, S.A., El-Gendy, N.S., El-Azab, W.I., Moustafa, Y.M., 2014. Kinetic, isotherm, and thermodynamic studies of polycyclic aromatic hydrocarbons biosorption from petroleum refinery wastewater using spent waste biomass. *Desalin. Water Treat.* 56, 3013–3023. <https://doi.org/10.1080/19443994.2014.964331>.
- Yu, L., Han, M., He, F., 2017. A review of treating oily wastewater. *Arab. J. Chem.* 10, 1913–1922. <https://doi.org/10.1016/j.arabjc.2013.07.020>.
- Yuan, P., Li, X., Wang, W., Liu, H., Yan, Y., Yang, H., Yue, Y., Bao, X., 2018. Tailored design of differently modified mesoporous materials to deeply understand the adsorption mechanism for PAHs. *Langmuir* 34, 15708–15718. <https://doi.org/10.1021/acs.langmuir.8b03299>.
- Zarei, M., Seyedi, N., Maghsoudi, S., Nejad, M.S., Sheibani, H., 2021. Green synthesis of Ag nanoparticles on the modified graphene oxide using *Capparis spinosa* fruit extract for catalytic reduction of organic dyes. *Inorg. Chem. Commun.* 123, 108327. <https://doi.org/10.1016/j.inoche.2020.108327>.
- Zhang, B., 2018. Introduction. In: Zhang, B. (Ed.), *Physical Fundamentals of Nanomaterials*. Elsevier Inc, China, pp. 1–18.
- Zhang, C., Wu, L., Cai, D., Zhang, C., Wang, N., Zhang, J., Wu, Z., 2013. Adsorption of polycyclic aromatic hydrocarbons (Fluoranthene and Anthracenemethanol) by functional graphene oxide and removal by pH and temperature-sensitive coagulation. *Appl. Mater. Interfaces* 5, 4783–4790. <https://doi.org/10.1021/am4002666>.
- Zhang, J., Li, R., Ding, G., Wang, Y., Wang, C., 2019. Sorptive removal of phenanthrene from water by magnetic carbon nanomaterials. *J. Mol. Liq.* 293, 111540. <https://doi.org/10.1016/j.molliq.2019.111540>.
- Zhang, Y., Wu, B., Xu, H., Liu, H., Wang, M., He, Y., Pan, B., 2016. Nanomaterials-enabled water and wastewater treatment. *NanoImpact* 3–4, 22–39. <https://doi.org/10.1016/j.impact.2016.09.004>.
- Zhao, C., Zhou, J., Yan, Y., Yang, L., Xing, G., Li, H., Wu, P., Wang, M., Zheng, H., 2021. Application of coagulation/flocculation in oily wastewater treatment: A review. *Sci. Total Environ.* 765, 142795. <https://doi.org/10.1016/j.scitotenv.2020.142795>.